MYCOLOGY
2025, VOL. 16, NO. 1, 124–157
https://doi.org/10.1080/21501203.2024.2410508

Taylor & Francis
Taylor & Francis Group

RESEARCH ARTICLE

OPEN ACCESS Check for updates

Catalogue of fungi in China 4: Didymiaceae and Physaraceae (Myxomycetes)

Xuefei Li[a,b], Jiajun Hu[a,c], Yonglan Tuo[a,b], You Li[a], Dan Dai[a,d], Frederick Leo Sossah[a,e], Minghao Liu[b], Jiajia Wang[a,b], Jiage Song[f], Bo Zhang[a,b], Xiao Li[a,b] and Yu Li[a,b]

[a]Engineering Research Center of Chinese Ministry of Education for Edible and Medicinal Fungi, Jilin Agricultural University, Changchun, China; [b]College of Mycology, Jilin Agricultural University, Changchun, China; [c]School of Life Science, Zhejiang Normal University, Jinhua, China; [d]Institute of Agricultural Applied Microbiology, Jiangxi Academy of Agricultural Sciences, Nanchang, China; [e]Council for Scientific and Industrial Research (CSIR), Oil Palm Research Institute, Coconut Research Programme, Sekondi, Ghana; [f]Innovative Institute for Plant Health/Key Laboratory of Green Prevention and Control on Fruits and Vegetables in South China, Ministry of Agriculture and Rural Affairs, Zhongkai University of Agriculture and Engineering, Guangzhou, China

ABSTRACT

Myxomycetes play crucial ecological roles, yet their species diversity, distribution, and taxonomic relationships remain poorly understood. In this study, we examined 104 specimens from 19 provinces in China. Through morphological analysis, we identified a group of species with reduced lime formation, a feature typically associated with the Physaraceae, but with key morphological similarities to the *Diderma*. A comprehensive phylogenetic analysis was conducted using three genes (nSSU, *EF-1α*, and *COI*), resulting in a dataset of 452 sequences from 116 species. Notably, we identified a distinct clade within Didymiaceae containing species with fewer lime knots, a trait traditionally linked to Physaraceae. This clade, designated as the new genus *Neodiderma*, was phylogenetically positioned as a sister group to *Diderma*, potentially representing a transitional group between Didymiaceae and Physaraceae, supported by both morphological and molecular evidence. Eleven new species — *N. macrosporum*, *N. pseudobisporum*, *N. verrucocapillitium*, *N. rigidocapillitium*, *N. rufum*, *Physarum guangxiense*, *P. subviride*, *P. nigritum*, *P. biyangense*, *P. neoovoideum*, and *P. jilinense* — were identified from China, and their phylogenetic positions were analysed. Additionally, *N. spumarioides* (formerly *Diderma spumarioides*) was recombined. The new and recombined species were formally described and illustrated, and a key to the sections and species of *Neodiderma* and *Physarum* was provided.

ARTICLE HISTORY
Received 24 July 2024
Accepted 24 September 2024

KEYWORDS
New taxa; phylogenetic analysis; taxonomy; slime mould

1. Introduction

Myxomycetes are an important component of terrestrial ecosystems, playing a crucial role in biodiversity conservation (Stephenson et al. 2008; Liu et al. 2024). Among the various genera of myxomycetes, *Diderma* Pers. and *Physarum* Pers. stand out for their abundance and ecological significance. Both genera typically thrive in moist and shaded environments, obtaining nutrients from substrates such as dead leaves, mosses, and decaying stumps. While they can adapt to a variety of vegetation types and environmental conditions, they show a preference for these specific habitats.

Traditionally, *Diderma* species are characterised by sporocarps containing irregularly shaped lime granules, which are distributed in different patterns depending on the species. Most *Diderma* species are sessile and have a distinctive peridium, which can be single- to triple-layered and contains globular lime granules. These granules may vary range from brittle and calcareous to flexible and cartilaginous. *Diderma* usually has a columella present, and its capillitium lacks lime nodes. In contrast, *Physarum* species are characterised by stipitate sporocarps, though they can occasionally be sessile. The stalk often lacks lime and the columella is absent. *Physarum*'s capillitium is connected with lime knots, and its spores are free. One key feature that distinguishes *Diderma* from other species in the family Physaraceae is the absence of lime knots in its non-calcareous capillitium (Chow 1977; García-Martín et al. 2023). Recently, García-Martín et al. (2023) revised the taxonomic framework of the order Physarales and updated definitions for several genera. They established the new genus *Nannengaella* from species previously classified under

CONTACT Bo Zhang zhangbofungi@126.com; Xiao Li lxmogu@163.com; Yu Li yuli966@126.com Engineering Research Center of Chinese Ministry of Education for Edible and Medicinal Fungi, Jilin Agricultural University, Changchun 130118, China

This article has been corrected with minor changes. These changes do not impact the academic content of the article.

Physarum that have heavily calcified sporophores and often a true calcareous columella (García-Martín et al. 2023).

The taxonomic status of the genera *Diderma* and *Physarum* has long been debated. In 1873, Rosafinski established the family Physaraceae, emphasising lime as a key taxonomic criterion for myxomycetes within the family and placed *Diderma* in the family Didymiaceae (Rostafiński 1873; Chow 1977; Li et al. 2008). However, in 1925, Lister reclassified *Diderma* within Physaraceae (Lister 1925). Later, Martin and Alexopoulos (1969) proposed a classification that returned *Diderma* to Didymiaceae, a view that remained accepted for many years (Martin and Alexopoulos 1969). More recent studies by Nandipati et al. (2012), Leontyev et al. (2019), and Cainelli et al. (2020) observed that the family Physaraceae forms a monophyletic clade, with *Diderma* positioned as a sister branch. García-Martín et al. (2023) have since provided further evidence supporting *Diderma*'s classification within Didymiaceae, reigniting the taxonomic debate surrounding this genus. Given this ongoing controversy, it is hypothesised that *Diderma* or related genera may represent transitional links between the evolutionary lineages of the families Didymiaceae and Physaraceae.

Research on the classification and diversity of myxomycetes in China began relatively late. However, through long-term species surveys and specimen collection, significant progress has been made in the modern myxomycetes taxonomy, greatly enhancing our understanding of species distribution patterns in China and worldwide. Currently, nearly 500 species of myxomycetes have been documented in China, representing about half of the approximately 1,100 known species globally (Rao and Chen 2023; Lado 2024). Of these, the genus *Diderma* includes 94 species worldwide, with 37 species reported in China, accounting for approximately 39.4% of the global total (Lado 2024; Li et al. 2024a, 2024b). The genus *Physarum* has 145 species worldwide, with 71 species found in China, representing about 49% of the known species (Chen et al. 2012; García-Martín et al. 2023; Lado 2024). Given China's vast territory, rich natural resources, and diverse ecological environment, many more myxomycetes species likely remain undiscovered.

This study confirmed the existence of 11 new species, including five from the genus *Neodiderma* and six from the genus *Physarum*. Phylogenetic analyses, incorporating molecular data from most of the known global species, revealed that five of these new species, along with one reclassified species, form the distinct genus *Neodiderma*. *Neodiderma* is positioned as a transitional genus between the families Didymiaceae and Physaraceae. These findings significantly improve our understanding of species diversity within Didymiaceae and Physaraceae in China, while also clarifying taxonomic relationships among infrageneric taxa.

2. Materials and methods

2.1. Morphological studies

We observed 104 specimens collected from 19 provinces from 1980 to 2023, China. The examined collections have been deposited in the Herbarium of Mycology at Jilin Agriculture University (HMJAU), China.

Macroscopic characteristics were observed using a Zeiss dissecting microscope (Axio Zoom V16, Carl Zeiss Microscopy GmbH, Göttingen, Germany), and photographs were taken with a Leica stereoscopic dissector (Leica M165, Wetzlar, Germany). Specimens were dried and stored in the Herbarium of Mycology at Jilin Agriculture University (HMJAU). Colour terminology follows the Flora of British Fungi: Colour Identification Chart (Royal and Edinburgh 1969). Microscopic observations were conducted on tissue sections stained with 95% ethanol and 3% KOH under a light microscope (Axio Imager A2, Carl Zeiss Microscopy GmbH, Göttingen, Germany) at magnifications up to 1,000× (total magnification of eyepiece and objective). All measurements were made in 3% KOH. The variation in sporocarpic and spore diameters is now presented as (minimum–) 25th percentile – 75th percentile (–maximum), which accurately delineates spore dimensions (Leontyev et al. 2023; Song and Chen 2024). Specifically, we measured the diameters of 10 sporothecae, sporocarpic structures, and stalks. Additionally, 20 spores were measured, with ornamentation included. For scanning electron microscopy (SEM) observations, air-dried sporocarps were mounted on a holder and sputtered with gold using a Hitachi E-1010 sputter coater. The microscopic

characteristics of the capillitium, spores, and lime granules on the surface of the peridium were examined with a Hitachi S-4800 SEM (Japan) at 5–10 kV (Zhang et al. 2020).

2.2. DNA extraction, PCR amplification, and sequencing

Genomic DNA was extracted from voucher specimens using the TIANamp Micro DNA Kit (TianGen Biotech Co., Ltd., Beijing, China), following the manufacturer's instructions. For amplification of the nuclear small subunit ribosomal RNA (nSSU), translation elongation factor 1-alpha (*EF-1α*), and mitochondrial cytochrome c oxidase subunit I (*COI*) genes, we used specific primer pairs: SSU101F/P1R (Wang et al. 2021) for nSSU, PB1F/PB1R (Novozhilov et al. 2013) for *EF-1α*, and COMF/COMRs (Feng and Schnittler 2015; Liu et al. 2015; Novozhilov et al. 2019) for *COI*. Polymerase chain reactions (PCR) were conducted in a total volume of 25 µL, comprising 2 µL template DNA, 8.5 µL distilled water, 1 µL of each primer (10 µmol/L), and 12.5 µL 2× PCR mix (TransGen Biotech Co., Ltd., Beijing City, China).

Amplification reactions were performed under the following conditions: for nSSU amplification, initial denaturation at 95 °C for 6 min, followed by 32 cycles of 95 °C for 1 min, 52 °C for 1 min, and 72 °C for 1 min, with a final extension at 72 °C for 10 min; for *EF-1α* amplification, initial denaturation at 95 °C for 5 min, followed by 36 cycles of 95 °C for 30 s, 65.4 °C for 30 s, and 72 °C for 1 min, with a final extension at 72 °C for 10 min (Novozhilov et al. 2013); for *COI* amplification using the COMF/COMRs primer pair, initial denaturation at 95 °C for 5 min, followed by 36 cycles of 95 °C for 30 s, 52 °C for 20 s, and 72 °C for 1 min, with a final extension at 72 °C for 10 min. All PCR products were stored at 4 °C. Subsequently, the PCR products were electrophoresed on 1% agarose gels, and the purified products were sent to Kumei Biotechnology Co., Ltd. (Changchun City, China) for sequencing using the Sanger method. Newly generated sequences from this study were deposited in GenBank.

2.3. Phylogenetic analysis

Partial regions of nSSU, *EF-1α*, and *COI* were amplified from 32 specimens, with corresponding herbarium numbers and GenBank accession numbers listed in Table 1. Additionally, 390 sequences from closely related species were retrieved from GenBank for phylogenetic comparison (Table 1). Sequence alignment was initially done using BioEdit 7.1.3 (Hall 1999) and Clustal X 1.81 (Thompson et al. 1997; Hall 1999), followed by multiple alignments using MAFFT 7.471 (Katoh and Standley 2013), employing the "auto" option with default gap penalties in PhyloSuite 1.2.3 (Zhang et al. 2020). Separate phylogenetic analyses were conducted for each marker gene, and the resulting topologies were visually inspected for congruence. A partition homogeneity test (PAUP 4.0, Goloboff et al. 2022) was used to assess the compatibility of marker sequences, and based on satisfactory congruence, the sequences were concatenated for the final phylogenetic analysis.

Both Bayesian Inference (BI) and Maximum Likelihood (ML) methods were employed to construct phylogenetic trees. The best-fit substitution models were selected using the Bayesian Information Criterion (BIC) in ModelFinder (Kalyaanamoorthy et al. 2017). For the ML analysis, IQTREE 1.6.12 (Nguyen et al. 2015) was used, with 1,000 ultrafast bootstrap support (UBS) replicates to generate confidence values for clades. For the Bayesian analysis, posterior probabilities (PPs). Bayesian analysis was conducted using Markov Chain Monte Carlo (MCMC) sampling in MrBayes (Ronquist et al. 2012). A total of 5,000,000 generations were run with trees sampled every 1,000 generations, using eight heated and one cold Markov chain, and the initial 25% of samples were discarded as burn-in.

The optimal nucleotide substitution models for BI phylogeny were GTR + F + I + G4 for both nSSU and *COI*, and SYM + I + G4 for *EF-1α*. For the ML analysis, the best models were GTR + F + R5 for nSSU and *EF-1α*, and GTR + F + I + G4 for *COI*. A comparison of the topologies from both BI and ML analyses revealed nearly identical results. The final phylogenetic trees were visualised using ITOL version 6.9 (Bork 2007), and branch support values were automatically displayed. Details of reference strains are provided in Table 1.

3. Results

3.1. Molecular phylogeny

The combined three-gene dataset (nSSU + *EF-1α* + *COI*) included sequences from 220 samples representing 116 taxa. This dataset utilised a total of 452

Table 1. Taxa and GenBank accession numbers used in phylogenetic analysis.

Scientific name	Voucher/specimen numbers	GenBank accession numbers			Reference
		nSSU	*EF-1a*	*COI*	
Amaurochaete comata	AMFD171	AY842031	AY842029	–	Fiore-Donno et al. (2005)
Badhamia bethelii	MA-Fungi 42170	–	MW240121	–	García-Martín et al. (2023)
B. capsulifera	MM46034	OP646290	OP672394	–	García-Martín et al. (2023)
B. capsulifera	MM33768	OP646288	OP631009	–	García-Martín et al. (2023)
B. foliicola	MA-Fungi 69058	KC759100	MG963465	–	Aguilar et al. (2014)
B. foliicola	MA-Fungi 34,660	MF352445	MF352491	–	García-Martín et al. (2018)
B. melanospora	MA-Fungi 81706	KC758975	MG963469	–	Aguilar et al. (2014)
B. melanospora	MA-Fungi 64653	KC759019	MG963468	–	Aguilar et al. (2014)
B. versicolor	MA-Fungi 78737	–	MW240024	–	García-Martín et al. (2023)
Comatricha nigra	MA-Fungi 86360	–	MW240026	–	García-Martín et al. (2023)
Craterium crateriachea	MM47834	OP646307	OP631031	–	García-Martín et al. (2023)
C. crateriachea	MM23006	–	OP631030	–	García-Martín et al. (2023)
C. aureum	MM29674	–	OP631017	–	García-Martín et al. (2023)
C. aureum	MM24280	–	OP631016	–	García-Martín et al. (2023)
C. minutum	MA-Fungi 91232	MG963643	MG963475	–	García-Martín et al. (2023)
C. minutum	MA-Fungi 62848	MF352455	MF352501	–	García-Martín et al. (2018)
C. roseum	MA-Fungi 81892	MW240392	MW240141	–	García-Martín et al. (2023)
C. roseum	MA-Fungi 41441	–	MW240140	–	García-Martín et al. (2023)
C. leucocephalum	MA-Fungi 69902	MG963641	MG963472	–	García-Martín et al. (2023)
C. leucocephalum	MA-Fungi 69800	MG963640	MG963471	–	García-Martín et al. (2023)
Diderma alpinum	sc30044	MN595463	MN596920	–	Shchepin et al. (2024)
D. alpinum	YK385	MN595608	OP616431	OP616538	Prikhodko et al. (2023)
D. annuliferum	HMJAU M20001-1	PP165419	PP178586	–	Li et al. (2024a)
D. annuliferum	HMJAU M20001-2	PP165420	PP178587	–	Li et al. (2024a)
D. clavatocolumellum	HMJAU 11084-1	PP165417	PP178585	PP261313	Li et al. (2024a)
D. clavatocolumellum	HMJAU 11084-2	PP165418	PP982177	PP261314	Li et al. (2024a)
D. chondrioderma	MYX439	KM977850	MK555282	–	Hoppe and Schnittler (2015)
D. deplanatum	MYX440	KM977851	MK555283	–	Hoppe and Schnittler (2015)
D. effusum	HMJAU M20014	PP165441	PP178601	–	Li et al. (2024a)
D. effusum	HMJAU M20015	PP165443	PP178603	PP261320	Li et al. (2024a)
D. effusum	MYX7994	MZ604987	MZ605416	OP616543	Novozhilov et al. (2022)
D. europaeum	MA-Fungi 73109	MG963656	MG963487	–	García-Martín et al. (2023)
D. europaeum	MA-Fungi 73112	MG963657	MG963488	–	García-Martín et al. (2023)
D. flexocapillitium	HMJAU M20020	PP165451	PP178608	–	Li et al. (2024a)
D. flexocapillitium	HMJAU M20022	PP165453	PP178610	–	Li et al. (2024a)
D. floriforme	MdH1810007	OM339175	–	–	Ronikier et al. (2022)
D. floriforme	MYX18793	OP621222	OP616432	OP616547	Prikhodko et al. (2023)
D. gansuense	HMJAU M20013-1	PP165439	PP178600	–	Li et al. (2024a)
D. gansuense	HMJAU M20013-2	PP165440	–	–	Li et al. (2024a)
D. globosum	LE325799	MZ604992	MZ605421	OP616551	Novozhilov et al. (2022)
D. globosum	LE325800	MZ604993	MZ605422	OP616552	Novozhilov et al. (2022)
D. globosum	HMJAU M20016	PP165444	PP178604	–	Li et al. (2024b)
D. hemisphaericum	HMJAU M20017	PP165445	–	–	Li et al. (2024a)
D. hemisphaericum	MA-Fungi 63960	MG963659	MG963490	–	García-Martín et al. (2023)
D. hemisphaericum	MA-Fungi 90974	MG963660	MG963491	–	García-Martín et al. (2023)
D. jilinense	HMJAU M20042	PP165482	PP178627	PP261327	Li et al. (2024a)
D. jilinense	HMJAU M20043	PP165483	PP178628	–	Li et al. (2024a)
D. meyerae	LE284739	KU198050	KU198109	–	Shchepin et al. (2024)
D. meyerae	sc30279	MN595488	MN596919	–	Shchepin et al. (2024)
D. niveum	MA-Fungi 78779	MW240312	MW240041	–	García-Martín et al. (2023)
D. niveum	MA-Fungi 78780	MW240313	–	–	García-Martín et al. (2023)
D. pseudotestaceum	LE291396	KJ659866	KJ676604	–	Novozhilov et al. (2014)
D. pseudotestaceum	LE291397	KJ659867	KJ676605	–	Novozhilov et al. (2014)
D. radiatum	MYX9867	MZ604983	MZ605412	OP616561	Novozhilov et al. (2022)
D. radiatum	MYX9071	MK838444	MZ605410	OP616560	Novozhilov et al. (2022)
D. roanense	HMJAU M20002	PP165421	–	PP261315	Li et al. (2024a)
D. roanense	HMJAU 8877	PP165423	–	–	Li et al. (2024a)
D. roanense	HMJAU M20003	PP165424	PP178588	–	Li et al. (2024a)
D. roseum	HMJAU M20046	PP165486	PP178631	–	Li et al. (2024a)
D. roseum	HMJAU M20047	PP165487	PP178632	–	Li et al. (2024a)
D. roseum	HMJAU M20048	PP165488	PP178633	–	Li et al. (2024a)
D. saundersii	HMJAU M20027-1	PP165461	PP178616	PP261323	Li et al. (2024a)
D. saundersii	HMJAU M20027-2	PP165462	PP178617	–	Li et al. (2024a)
D. shaanxiense	HMJAU M20033	PP165469	PP178624	PP261324	Li et al. (2024b)
D. shaanxiense	HMJAU M20034	PP165470	–	PP261325	Li et al. (2024b)
D. testaceum	HMJAU M20029	PP165463	PP178618	–	Li et al. (2024a)
D. testaceum	HMJAU M20030	PP165465	PP178620	–	Li et al. (2024a)
D. velutinum	LE318752	MH714785	MH717084	MH717086	Bortnikov et al. (2018)
D. velutinum	LE318753	MH714786	MH717085	MH717087	Bortnikov et al. (2018)
D. verrucocapillitia	HMJAU M20032-1	PP165467	PP178622	–	Li et al. (2024a)

(*Continued*)

Table 1. (Continued).

Scientific name	Voucher/specimen numbers	GenBank accession numbers			Reference
		nSSU	*EF-1a*	*COI*	
D. verrucocapillitia	HMJAU M20032-2	PP165468	PP178623	–	Li et al. (2024a)
Diachea subsessilis	MA-Fungi 68835	ON059426	–	–	Lado et al. (2022)
D. subsessilis	MA-Fungi 60512	MW240302	MW240030	–	García-Martín et al. (2023)
D. mitchellii	MA-Fungi 91212	ON059421	ON081607	–	Lado et al. (2022)
D. mitchellii	MA-Fungi 96696	ON059424	ON081610	–	Lado et al. (2022)
D. leucopodia s. lat.	MA-Fungi 86466	MG963645	MG963477	–	García-Martín et al. (2023)
D. leucopodia s. lat.	MA-Fungi 86465	MG963644	MG963476	–	García-Martín et al. (2023)
D. silvaepluvialis	MA-Fungi 51360	ON059425	–	–	Lado et al. (2022)
D. dictyospora	MM39407	OP646293	OP631018	–	García-Martín et al. (2023)
D. muscorum	MM28650	OP646294	OP631011	–	García-Martín et al. (2023)
D. obovata	MM39542	OP646296	–	–	García-Martín et al. (2023)
D. obovata	MM37196	OP646295	–	–	García-Martín et al. (2023)
Didymium azorellae	MA-Fungi 90715	MW240317	MW240045	–	García-Martín et al. (2023)
D. azorellae	MA-Fungi 91159	MW240316	MW240046	–	García-Martín et al. (2023)
D. clavus	MA-Fungi 81623	MW240321	MW240051	–	García-Martín et al. (2023)
D. clavus	MA-Fungi 69756	MW240320	MW240050	–	García-Martín et al. (2023)
D. comatum	MA-Fungi 34607	–	MW240052	–	García-Martín et al. (2023)
D. difforme	MA-Fungi 83652	MG662515	MW240057	–	García-Martín et al. (2023)
D. difforme	MA-Fungi 64529	MW240323	MW240054	–	García-Martín et al. (2023)
D. dubium	MA-Fungi 80036	MW240327	MW240059	–	García-Martín et al. (2023)
D. dubium	MA-Fungi 80492	MG662512	MW240060	–	García-Martín et al. (2023)
D. dubium	K7	AM231294	–	–	Wikmark et al. (2007)
D. exminum	MA-Fungi 64221	MW240330	–	–	García-Martín et al. (2023)
D. exminum	MA-Fungi 82049	MW240331	MW240063	–	García-Martín et al. (2023)
D. infundibuliforme	MA-Fungi 90840	MW240333	MG963495	–	García-Martín et al. (2023)
D. infundibuliforme	MA-Fungi 78324	MG963664	MW240065	–	García-Martín et al. (2023)
D. leptotrichum	MA-Fungi 83181	MW240334	MW240066	–	García-Martín et al. (2023)
D. melanospermum	MA-Fungi 91238	MG963668	MG963497	–	García-Martín et al. (2023)
D. melanospermum	MA-Fungi 62790	MG963667	MW240068	–	García-Martín et al. (2023)
D. minus	MA-Fungi 42163	MG963666	MG963496	–	García-Martín et al. (2023)
D. nivicola	MA-Fungi 90573	MT227090	MT230925	–	Janik et al. (2020)
D. nivicola	AH19667	MT227019	MT230908	–	Janik et al. (2020)
D. operculatum	MA-Fungi 74050	MG963669	MG963498	–	García-Martín et al. (2023)
D. operculatum	MA-Fungi 80820	MG963670	MW240070	–	García-Martín et al. (2023)
D. pertusum	MA-Fungi 69001	MW240337	MW240072	–	García-Martín et al. (2023)
D. pertusum	MA-Fungi 69000	MW240336	MW240071	–	García-Martín et al. (2023)
D. pseudonivicola	MA-Fungi 90601	MT227112	MT230931	–	Janik et al. (2020)
D. pseudonivicola	MA-Fungi 90587	MT227099	MT230927	–	Janik et al. (2020)
D. spongiosum	USA69766	MK649929	MK905758	–	Zhao et al. (2021)
D. spongiosum	MA-Fungi 82547	MW240367	MW240108	–	García-Martín et al. (2023)
D. squamulosum s. lat.	MA-Fungi 80292	MW240339	MW240074	–	García-Martín et al. (2023)
D. squamulosum s. lat.	HMJAU M3007	MF149873	MK905761	–	Zhao et al. (2021)
D. squamulosum s. lat.	MA-Fungi 82075	MW240341	MW240076	–	García-Martín et al. (2023)
D. tehuacanense	MA-Fungi 73605	MG963671	KJ545562	–	García-Martín et al. (2023)
D. tehuacanense	MA-Fungi 79152	MW240342	–	–	García-Martín et al. (2023)
D. umbilicatum	MA-Fungi 64629	MG963673	MW240077	–	García-Martín et al. (2023)
D. umbilicatum	MA-Fungi 64297	MG963672	MG963501	–	García-Martín et al. (2023)
D. yulii	HMJAU M3002	MF149871	MK905755	–	Zhao et al. (2021)
D. yulii	HMJAU M3001	MF149870	MK905754	–	Zhao et al. (2021)
Enerthenema intermedium	MM 21635	DQ903688	–	–	Fiore-Donno et al. (2008)
E. melanospermum	MM 28388	DQ903689	–	–	Fiore-Donno et al. (2008)
E. papillatum	AMFD141	AY643823	–	–	Fiore-Donno et al. (2005)
Lamproderma aeneum	MA-Fungi 81947	MW240352	MW240092	–	García-Martín et al. (2023)
Fuligo leviderma	MYX8341	MW692992	MW701630	–	Shchepin et al. (2022)
F. leviderma	MOROZ221	MW692991	MW701629	–	Shchepin et al. (2022)
F. luteonitens	MM47551	OP646302	OP631023	–	García-Martín et al. (2023)
F. luteonitens	MM47217	OP646301	OP631022	–	García-Martín et al. (2023)
F. septica	MA-Fungi 56967	–	MW240088	–	García-Martín et al. (2023)
F. septica	MA-Fungi 62772	–	MW240090	–	García-Martín et al. (2023)
F. septica	MA-Fungi 60076	MW240349	MW240089	–	García-Martín et al. (2023)
F. septica	MA-Fungi 78801	MF352459	MF352505	–	García-Martín et al. (2018)
F. septica	MA-Fungi 78118	MW240350	MW240091	–	García-Martín et al. (2023)
L. aeneum	MA-Fungi 86925	MW240353	MW240093	–	García-Martín et al. (2023)
L. aeneum	MA-Fungi 90422	MW240354	MW240094	–	García-Martín et al. (2023)
L. ovoideum	Sc30802	MN595543	MN596918	–	Shchepin et al. (2024)
Macbrideola oblonga	M. Schnittler	DQ903682	–	–	Fiore-Donno et al. (2008)
Meriderma aggregatum	AMFD135	DQ903669	–	–	Fiore-Donno et al. (2008)
M. carestiae var. *retisporum*	AMFD173	DQ903671	–	–	Fiore-Donno et al. (2008)
M. fuscatum	MM 24907	DQ903668	–	–	Fiore-Donno et al. (2008)
Nannengaella alpina	Sc29903	MH930698	MW701648	–	Shchepin et al. (2019)

(*Continued*)

Table 1. (Continued).

Scientific name	Voucher/specimen numbers	GenBank accession numbers			Reference
		nSSU	*EF-1a*	*COI*	
N. alpina	Sc29908	MW693002	MW701649	–	Shchepin et al. (2022)
N. alpina	Sc29955	MW693003	MW701650	–	Shchepin et al. (2022)
N. contexta	MA-Fungi 68752	MF352473	MF352522	–	García-Martín et al. (2018)
N. contexta	MA-Fungi 73321	MF352474	MF352523	–	García-Martín et al. (2018)
N. globulifera	MA-Fungi 51647	MF352479	MF352528	–	García-Martín et al. (2018)
N. globulifera	MA-Fungi 51815	–	MW240128	–	García-Martín et al. (2023)
N. mellea	MA-Fungi 69850	MF352484	MF352534	–	García-Martín et al. (2018)
N. mellea	MA-Fungi 87986	MF352485	MF352535	–	García-Martín et al. (2018)
N. mellea	MA-Fungi 60322	MW240383	MG963528	–	García-Martín et al. (2023)
N. mellea	MA-Fungi 60314	–	MG963527	–	García-Martín et al. (2023)
Neodiderma macrosporum	**HMJAU M20035-1**	**PP165471**	**PP178625**	**PP261326**	**This study**
N. macrosporum	**HMJAU M20035-2**	**PP165472**	**PP178626**	–	**This study**
N. macrosporum	**HMJAU M20035-3**	**PP165473**	**PP982091**	–	**This study**
N. macrosporum	**HMJAU M20036**	**PP165474**	–	–	**This study**
N. macrosporum	**HMJAU M20037**	**PP165475**	–	–	**This study**
N. macrosporum	**HMJAU M20038**	**PP165476**	–	–	**This study**
N. ochraceum	sc24091	MZ604997	MZ605426	OP616557	Novozhilov et al. (2022)
N. ochraceum	sc24049	MZ604996	MZ605425	OP616556	Novozhilov et al. (2022)
N. pseudobisporum	**HMJAU M20025-1**	**PP165457**	**PP178612**	–	**This study**
N. pseudobisporum	**HMJAU M20025-2**	**PP165458**	**PP178613**	–	**This study**
N. rigidocapillitium	**HMJAU M20023-1**	**PP165454**	**PP178611**	–	**This study**
N. rigidocapillitium	**HMJAU M20023-2**	**PP165455**	**PP948834**	–	**This study**
N. rufum	**HMJAU 60242-1**	**PP165456**	–	–	**This study**
N. rufum	**HMJAU 60242-2**	**PP951403**	–	–	**This study**
N. spumarioides	**HMJAU 11078-1**	**PP210629**	–	–	**This study**
N. spumarioides	**HMJAU 11078-2**	**PP210630**	–	–	**This study**
N. spumarioides	**HMJAU M20028**	**PP210631**	–	–	**This study**
N. spumarioides	MCCNNU2749	MG696639	–	–	Gao et al. (2018)
N. verrucocapillitium	**HMJAU M20039-1**	**PP165477**	–	–	**This study**
N. verrucocapillitium	**HMJAU M20039-2**	**PP165478**	–	–	**This study**
N. verrucocapillitium	**HMJAU M20039-3**	**PP165479**	–	–	**This study**
N. verrucocapillitium	**HMJAU M20040**	**PP165480**	–	–	**This study**
N. verrucocapillitium	**HMJAU M20041**	**PP165481**	–	–	**This study**
Physarum album s. lat.	LE286368	MW692999	MW701642	–	Shchepin et al. (2022)
P. album s. lat.	LE286342	MH930708	MW701641	–	Shchepin et al. (2019)
P. atacamense	MA_Fungi_87942	MW240374	MW240117	–	García-Martín et al. (2023)
P. atacamense	MA_Fungi_88415	MG963684	MG963518	–	García-Martín et al. (2023)
P. biyangense	**HMJAU M20349-1**	**PP951388**	**PP948809**	–	**This study**
P. biyangense	**HMJAU M20349-2**	**PP951389**	**PP948810**	–	**This study**
P. bogoriense	MA-Fungi 57191	MF352470	MF352516	–	García-Martín et al. (2018)
P. bogoriense	MA-Fungi 69863	MG963685	MG963519	–	García-Martín et al. (2023)
P. cinereum	MA-Fungi 63822	–	MF352517	–	García-Martín et al. (2018)
P. cinereum	MA-Fungi 70925	–	MF352519	–	García-Martín et al. (2018)
P. guangxiense	**HMJAU M20344-1**	**PP951409**	**PP948811**	–	**This study**
P. guangxiense	**HMJAU M20344-2**	**PP951410**	**PP948812**	–	**This study**
P. hongkongense	MA-Fungi 60336	MW240380	OP650830	–	García-Martín et al. (2023)
P. hongkongense	HMJAU M10272	PP981549	PP981983	–	Unpublished
P. jilinense	**HMJAU M20367-1**	**PP951401**	**PP948832**	–	**This study**
P. jilinense	**HMJAU M20367-2**	**PP951402**	**PP948833**	–	**This study**
P. didermoides	MA-Fungi 71195	MW240378	–	–	García-Martín et al. (2023)
P. didermoides	MA-Fungi 57262	MF352488	MF352542	–	García-Martín et al. (2018)
P. leucophaeum	MA-Fungi 49730	MG963686	MG963521	–	García-Martín et al. (2023)
P. leucophaeum	MA-Fungi 78861	MG963688	–	–	García-Martín et al. (2023)
P. leucophaeum	MA-Fungi 59323	MF352477	MF352526	–	García-Martín et al. (2018)
P. leucophaeum	MA-Fungi 81980	–	MW240131	–	García-Martín et al. (2023)
P. licheniforme	MA-Fungi 73290	MF352481	MF352530	–	García-Martín et al. (2018)
P. licheniforme	MA-Fungi 73293	MG963689	MG963524	–	García-Martín et al. (2023)
P. licheniforme	MA-Fungi 91208	MG963692	–	–	García-Martín et al. (2023)
P. licheniforme	MA-Fungi 91207	MG963691	MG963525	–	García-Martín et al. (2023)
P. neoovoideum	**HMJAU M20294-1**	**PP951386**	–	–	**This study**
P. neoovoideum	**HMJAU M20294-2**	**PP951387**	–	–	**This study**
P. nigritum	**HMJAU M21287-1**	**PP951379**	**PP948803**	**PP968031**	**This study**
P. nigritum	**HMJAU M21287-2**	**PP951380**	**PP948804**	**PP968032**	**This study**
P. nigritum	**HMJAU M20277-1**	**PP951381**	–	**PP968033**	**This study**
P. nigritum	**HMJAU M20277-2**	**PP981579**	–	**PP982120**	**This study**
P. nigritum	**HMJAU M20276-1**	**PP951382**	**PP948805**	–	**This study**
P. nigritum	**HMJAU M20276-2**	**PP951383**	**PP948806**	–	**This study**
P. nigritum	**HMJAU M20279-1**	**PP951384**	**PP948807**	–	**This study**
P. nigritum	**HMJAU M20279-2**	**PP951385**	**PP948808**	–	**This study**

(*Continued*)

Table 1. (Continued).

Scientific name	Voucher/specimen numbers	GenBank accession numbers			Reference
		nSSU	*EF-1α*	*COI*	
P. nivale	MA-Fungi 72831	MF352486	MF352536	–	García-Martín et al. (2018)
P. nivale	MA-Fungi 70191	MW240384	MG963529	–	García-Martín et al. (2023)
P. nivale	MA-Fungi 70193	MW240385	–	–	García-Martín et al. (2023)
P. polygonosporum	MA-Fungi 90740	MF352463	MF352509	–	García-Martín et al. (2018)
P. polygonosporum	MA-Fungi 90752	MW240387	–	–	García-Martín et al. (2018)
P. polygonosporum	MA-Fungi 90756	MW240390	MW240139	–	García-Martín et al. (2023)
P. polygonosporum	MA-Fungi 90742	MF352465	MF352510	–	García-Martín et al. (2018)
P. pseudonotabile s. lat.	LE255432	LT670439	KF250465	–	Borg Dahl et al. (2018)
P. pseudonotabile s. lat.	LE255437	LT670419	KC473813	–	Novozhilov et al. (2013); Borg Dahl et al. (2018)
P. pseudonotabile s. lat.	LE255703	LT670568	KF250468	–	Borg Dahl et al. (2018)
P. pseudonotabile s. lat.	LE284662	LT670428	KF250472	–	Borg Dahl et al. (2018)
P. psittacinum	HMJAU M20290	PP951393	PP948820	PP948844	Unpublished
P. psittacinum	HMJAU M20281	PP951395	PP948825	–	Unpublished
P. psittacinum	HMJAU M20323	PP951397	PP948822	PP948840	Unpublished
Physarum sp.	HMJAU M20358	PP981532	PP981968	–	Unpublished
Physarum sp.	HMJAU M20356	PP981530	PP981966	–	Unpublished
Physarum sp.	HMJAU M 20292	PP981590	PP982019	PP982131	Unpublished
Physarum sp.	HMJAU M 20285	PP981588	PP982017	PP982129	Unpublished
Physarum sp.	HMJAU M 20322	PP981596	PP982023	PP982135	Unpublished
Physarum sp.	HMJAU M 20280	PP981582	PP982011	PP982123	Unpublished
P. stellatum	LE297729	MW693019	MW701666	–	Shchepin et al. (2022)
P. stellatum	LE297741	MW693020	MW701667	–	Shchepin et al. (2022)
P. straminipes	MA-Fungi 90736	MF352490	MF352544	–	García-Martín et al. (2018)
P. straminipes	MA-Fungi 70363	MF352489	MF352543	–	García-Martín et al. (2018)
P. straminipes	MA-Fungi 87865	MW240394	–	–	García-Martín et al. (2023)
P. subviride	**HMJAU M10138-1**	**PP951415**	–	–	**This study**
P. subviride	**HMJAU M10138-2**	**PP951416**	–	–	**This study**
P. vernum	Sc30091	MW693021	MW701668	–	Shchepin et al. (2022)
P. vernum	Sc30257	MH930744	MW701669	–	Shchepin et al. (2019)
P. viride	LE302489	MW693022	MW701670	–	Shchepin et al. (2022)
P. viride	LE317322	MW693024	MW701672	OP616654	Shchepin et al. (2022); Prikhodko et al. (2023)
Stemonitis flavogenita	AMFD2005	AF239229	AY643819	–	Fiore-Donno et al. (2005)
Symphytocarpus impexus	–	AY230188	–	–	Walkera et al. (2003)

Sequences produced in this study are in bold.

sequences from three-gene loci (nSSU, *EF-1α*, and *COI*) to construct phylogenetic trees. Among these, 62 sequences were newly generated, consisting of 38 nSSU sequences, 19 *EF-1α* sequences, and 5 *COI* sequences (Figure 1). A total 12 species from 7 genera within the family Stemonitaceae were used as outgroups. The final dataset comprised 8,551 characters, including gaps, with 6,533 characters (including gaps) from nSSU, 1,235 characters from *EF-1α*, and 783 characters from *COI*. The Bayesian analysis ran for five million generations, yielding an average standard deviation of split frequencies of 0.006122, indicating a significant difference. Subsequently, the same dataset and alignment underwent analysis using the ML method. Phylogenetic trees constructed using both ML and BI methods showed similar topologies for the combined datasets. Finally, the ML analysis was chosen as the representative phylogeny. UBS ≥ 70% from the ML analysis and PP ≥ 0.90 (Figure 1).

The constructed phylogenetic tree shows two main branches: Didymiaceae and Physaraceae. Within Didymiaceae, four distinct genus-level clades are identifiable: the well-known genera *Diderma* Pers. *Diachea* Fr., and *Didymium* Schrad., and a newly identified genus-level clade recognised in this study, *Neodiderma* X.F. Li, B. Zhang & Y. Li. In the concatenated dataset phylogenetic tree, the *Neodiderma* clade appears as the sister clade to *Diderma*, with moderate support. This clade encompasses seven species: two previously known species, *N. ochraceum* (formerly *D. ochraceum*) and *N. spumarioides* (formerly *D. spumarioides*), and five new species, *N. rufum*, *N. macrosporum*, *N. pseudobisporum*, *N. rigidocapillitium*, and *N. verrucocapillitium* (Figure 1).

Within Physaraceae, there are five genera: *Nannengaella* J.M. García-Martín, J.C. Zamora & Lado, *Fuligo* Haller, *Badhamia* Berk., *Craterium* Trentep., and *Physarum* Pers. The *Physarum* genus includes six newly identified species. They are located on different branches and have significant genetic distances from known species, which are *P. guangxiense*, *P. subviride*, *P. nigritum*, *P. biyangense*, *P. neoovoideum*, and *P. jilinense*.

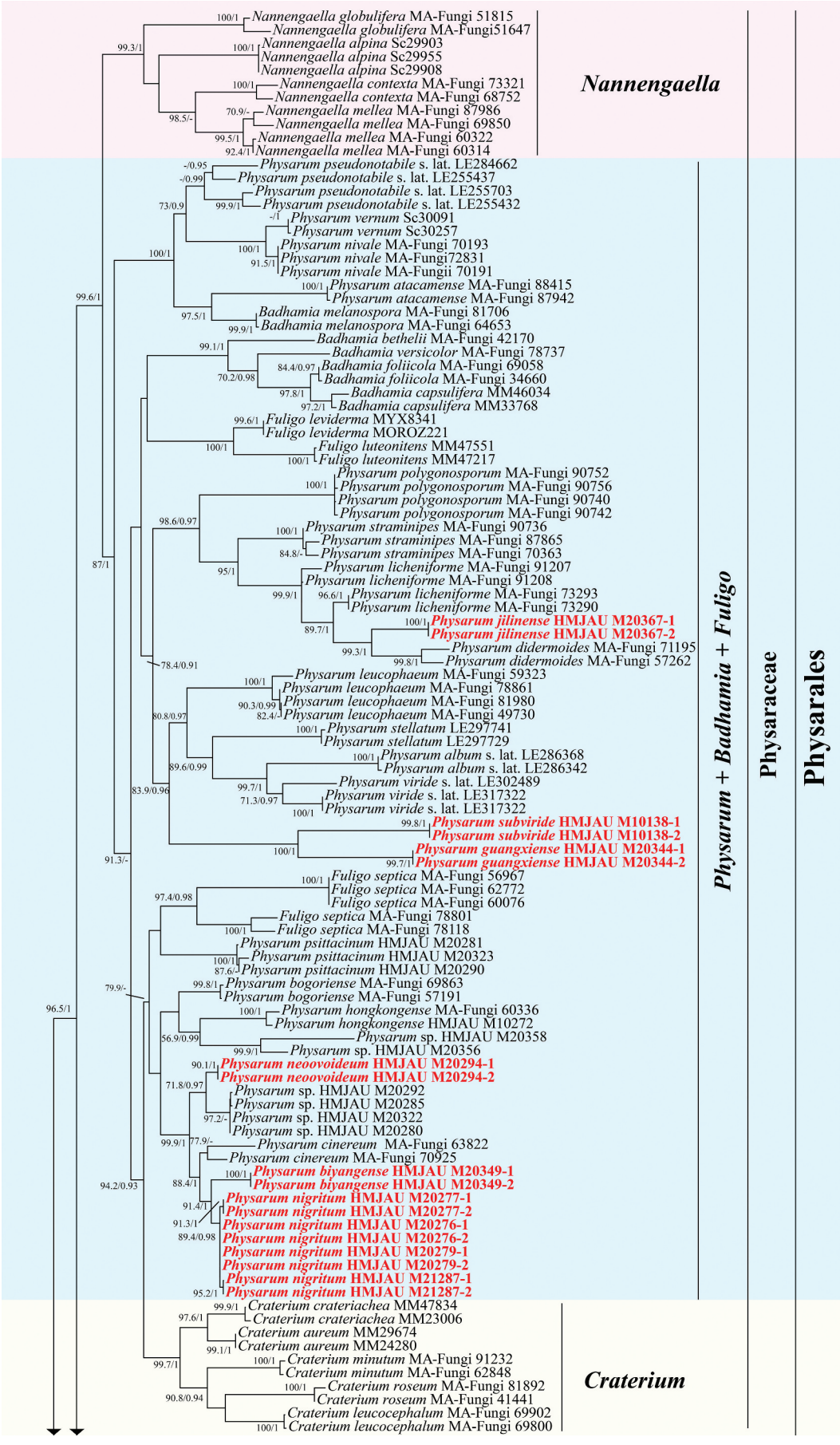

Figure 1. Phylogenetic tree diagram illustrating the evolutionary relationships between *Diderma* and *Neodiderma* in myxomycetes. This ML tree was constructed using the nSSU, *EF-1a*, and *COI* dataset. The values at the internal nodes represent the support from ML and BI analyses. UBS ≥ 70% from ML analysis and PP ≥ 0.90 are indicated on the branches. Newly sequenced collections are highlighted in bold, and newly discovered species are marked in red.

Figure 1. (Continued).

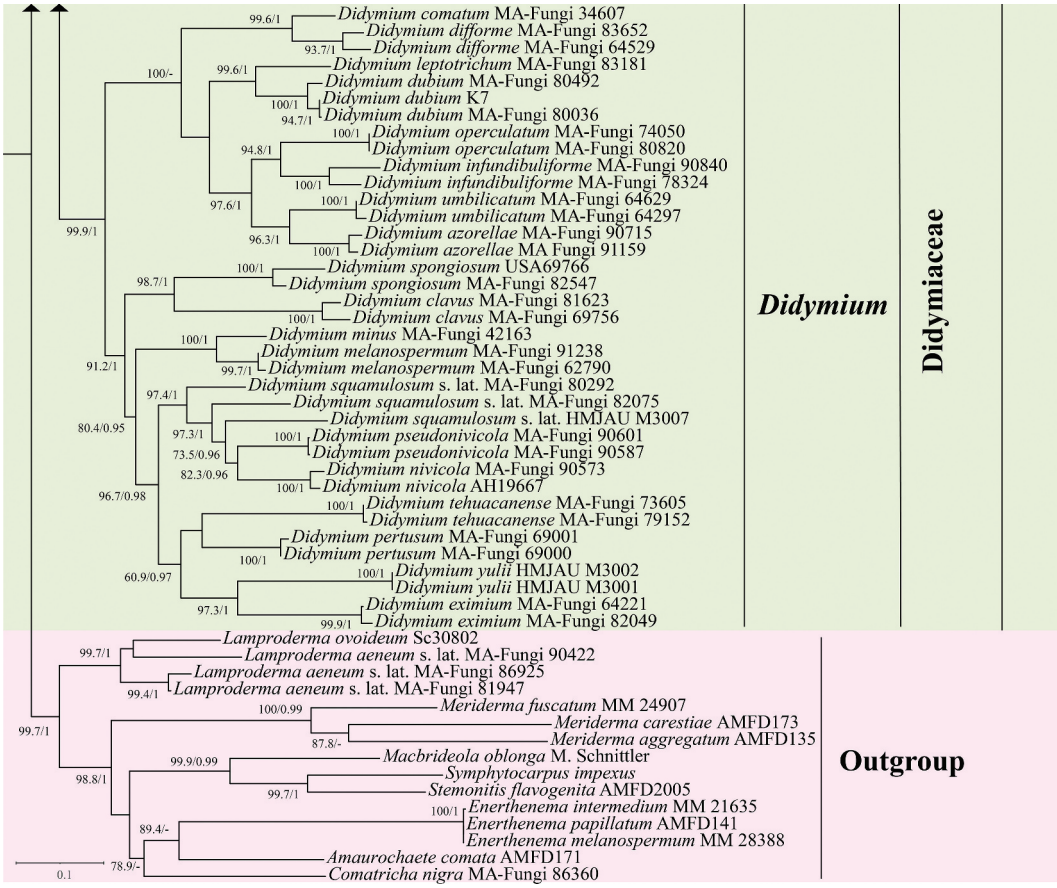

Figure 1. (Continued).

3.2. Taxonomy

Key to the genera in this study

1. Capillitium linear or dense network, connecting with lime knots.....2
1. Capillitium linear, branched and connected, lime free.....*Diderma*
2. Species have very less lime knots, difficult to observe, fusiform, brown .....*Neodiderma*
2. Species have obvious lime knots, variable shapes. Most parts of the sporophores containlimestone except for spores.....*Physarum*

Key to the species of genera *Neodiderma* present in this study

1. Large spores, spores >14 µm.....2
1. Small spores, spores <14 µm.....3
2. Capillitium dense network, wavy bending. Columella developed, irregular shape....*Neodiderma macrosporum*
2. Capillitium linear, hard and straight. Columella slightly convex, cushion.....*Neodiderma rigidocapillitium*
3. Spores with a deep groove in the middle, resembling two apposed hemispherical spores..... *Neodiderma pseudobisporum*
3. Spores without deep groove in the middle.....4
4. Peridium dark brown or red-brown.....*Neodiderma rufum*
4. Peridium white, ivory, or light grey.....5
5. Capillitium with more thickened nodules, columella light yellow brow.....*Neodiderma verrucocapillitium*
5. Capillitium with less thickened nodules, columella grey white.....*Neodiderma spumarioides*

Neodiderma X.F. Li, B. Zhang & Y. Li, gen. nov.
MycoBank: MB 852945.

Etymology: "*Neodiderma*" refers to this new genus similar to *Diderma*.

Diagnosis: Sporocarps frequently exhibit deformities due to mutual compression. The outer layer of the peridium is limy, white, or reddish-brown, while the columella features calcareous protrusions. The capillitium is brown and contains fewer lime nodes. The spore mass is dark brown.

Type: *Neodiderma macrosporum* X.F. Li, B. Zhang and Y. Li, sp. nov.

Description: Sporocarps, densely crowded, often stacked, and deformed due to mutual squeezing. Peridium typical two-layered, the outer layer calcareous, rough or smooth shells with amorphous lime granules loose or dense, the inner layer membranous, adheres closely or separates from the outer layer. Columella usually present, sometimes with a thickened at the sporotheca base. Capillitium linear, connecting with lime knots, and some species have very less lime knots, brown, rough, branching and connecting, with thickened nodules and enlarged membranous enlargement. Spores black or dark brown in mass, light brown by transmitted light (TL).

Notes: Morphologically, species within the genus *Neodiderma* exhibit a small number of lime nodes, and their main characteristics are similar to those of *Diderma*. Phylogenetic analysis indicates that *Neodiderma* forms a sister branch to *Diderma* and is classified as a distinct genus based on both morphological and phylogenetic evidence. To aid in distinguishing between the closely related species, we have provided a comprehensive comparison of their morphological features in Table 2. This table highlights the specific characteristics of each *Neodiderma* species, allowing for a clearer understanding of the differences among them.

Neodiderma macrosporum X.F. Li, B. Zhang & Y. Li, sp. nov. Figure 2

MycoBank: MB 852946.

Etymology: The epithet "*macrosporum*" refers to the big spores of the species.

Diagnosis: Sporocarps are densely packed, exhibiting a white colouration and distortion due to mutual pressure. The outer layer of the peridium is thick and covered with lime granules. The calcareous columella is fawn in colour, irregular in shape, and rough in texture, with some specimens occupying up to half of the sporotheca and varying in size. The capillitium contains lime nodes and large spores.

Table 2. Comparison of morphological characteristics of *Neodiderma* species.

Species name	Sporocarps	Peridium	Columella	Capillitium	Spores
N. macrosporum	Sessile, mutual extrusion deformation, (0.5–) 0.54–0.93 (–0.95) mm, white.	Double.	Developed, irregular shape, rough, varying in size, fawn.	Capillitium brown, with dark thickened and spindle shaped nodules, lime nodes yellow, less.	Spores with dense spiny, sometimes connected into ridges, (14–) 14.5–17 µm.
N. pseudobisporum	Sessile, buried deeply, (0.4–) 0.5–0.7 (–0.8) mm, white.	Double.	Hemispherical, white.	Capillitium brown, with dark brown swelling, lime nodes yellow, large, very less.	Spores with a deep groove in the middle, with warts and ridge, (11.5–)12–13 (–14) µm.
N. verrucocapillitium	Sessile, mutual extrusion deformation, (0.65–) 0.71–0.89 (–0.95) mm, white or pale-white.	Double.	Hemispherical protrusion at the base, light yellowish-brown.	Capillitium brown, dark thickened and spindle or subglobose shaped nodules, with yellow and spindle lime nodes.	Spores with sparse spiny, 8–9.5(–10) µm.
N. rigidocapillitium	Sessile, (0.6–) 0.63–0.82 (–0.85) mm, greyish black to greyish white, halo at the base.	Double, the outer layer easy to fall off.	Slightly convex, cushion, white or cream yellow, with limy, uneven.	Capillitium brown, with dark swellings and nodules, lime nodes yellow, large, very less.	Spores with shortly spiny, (11.5–)12–15(–16) µm.
N. rufum	Sessile, (0.3–) 0.32–0.77 (–0.8) mm, dark brown or reddish brown.	Double, smooth.	Protuberance, flat pulvinate, rusty brown or yellowish-brown.	Capillitium brown, lime nodes yellow, large, very less.	Spores ornamented with densely warts, (8.5–)9–10 µm.
N. spumarioides	Sessile, buried deeply, (0.35–) 0.4–0.8 (–0.85) mm, white or pale grey.	Double.	Rounded and convex, pulvinate or hemispherical, grey.	Capillitium brown, with small thickenings, lime nodes yellow, very less.	Spores with sparse spinules, (8.5–)9–10(–11) µm.

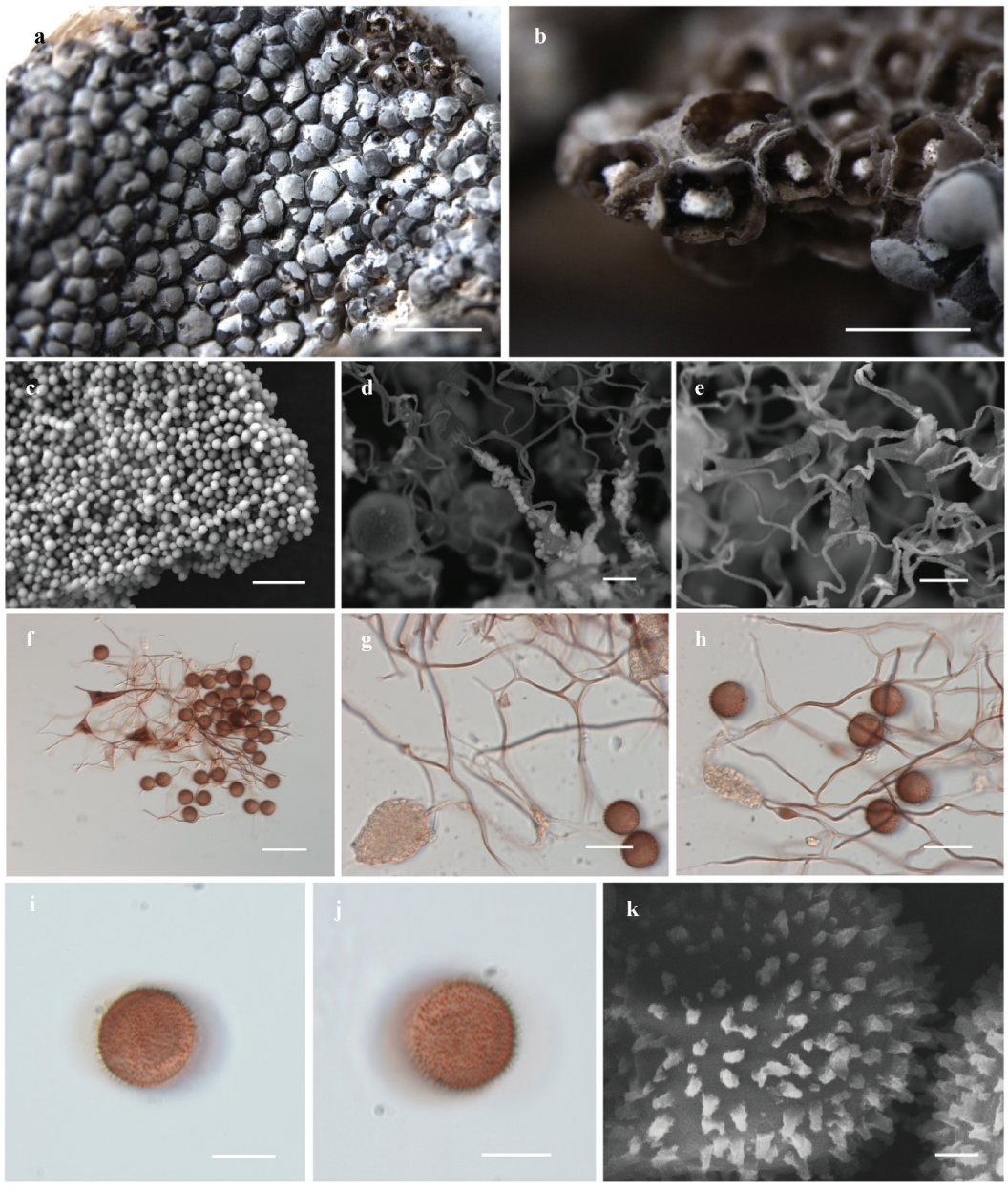

Figure 2. Habitat and microstructure of *Neodiderma macrosporum* (HMJAU M20035 holotype). (a, b) Sporocarps and columella. (c) Limestone on the outer surface of the peridium. (d) Lime nodes by SEM. (e) Capillitium by SEM. (f–h) Capillitium, spores and lime nodes by transmitted light (TL). (i–k) spores by TL and SEM. Scale bars: a = 2 mm; b = 1 mm; c = 10 µm; d = 5 µm; e = 100 µm; f = 40 µm; g, h = 20 µm; i, j = 10 µm; k = 1 µm.

Type: China, Inner Mongolia Autonomous Region, Hulunbuir City, 205 Management and Protection Station of Genhe Forestry Bureau, on the rotten leaves, 3 September 2021, B. Zhang (HMJAU M20035, holotype).

Description: Sporocarps, sessile, gregarious, spherical or hemispherical, stacking, often mutual extrusion deformation, (0.5–) 0.54–0.93 (–0.95) mm in diameter. Peridium typically double-layered, the outer layer calcareous, composed of a tightly packed layer of calcareous lime granules, white, the inner layer membranous, grey-white, often separated from the outer layer, sometimes wrinkled, irregular dehiscent, top retain, edge fall off. Columella developed, calcareous, fawn, irregular shape, rough, some occupying half of the sporotheca, varying in size. Hypothallus brown, membranous, transparent. Capillitium dense network, with yellow lime nodes, wavy and curved, brown, colourless at the end, many branches and with membrane enlargement sheet, dark thickened and spindle shaped nodules. Spore dark in

mass, reddish brown by TL, (14–) 14.5–17 µm in diameter, with dense spiny, sometimes connected into ridges. Plasmodium unknown.

Habitat: On the rotten leaves.

Distribution in China: Inner Mongolia Autonomous Region.

Distribution in the world: China.

Additional specimens examined: China, Inner Mongolia Autonomous Region, Hulunbuir City, 205 Management and Protection Station of Genhe Forestry Bureau, on the rotten leaves, 3 September 2021, B. Zhang (HMJAU M20036, HMJAU M20037, HMJAU M20038, HMJAU M20102, HMJAU M20103).

Notes: This species shares several morphological characteristics with those in the genus *Diderma* Pers., including subglobose sporocarps with smooth, amorphous lime granules, which may appear either loose or dense. The capillitium is brown and rough, characterised by thickened nodules and membranous enlargements. However, *Neodiderma macrosporum* can be distinguished from *Diderma* by its linear capillitium, which has fewer lime nodes. Additionally, the columella exhibits an irregular shape and varies in size. Phylogenetically, *Neodiderma macrosporum* forms a distinct clade that is sister to the genus *Diderma* (Figure 1). Furthermore, compared to other known species, *N. macrosporum* has notably larger spores, which further highlights its uniqueness.

Neodiderma pseudobisporum X.F. Li, B. Zhang & Y. Li, sp. nov. Figure 3

MycoBank: MB 852947.

Etymology: The epithet "*pseudobisporum*" refers to the spore-like two hemispherical spores apposed.

Diagnosis: Sporocarps are subglobose and exhibit angularity due to mutual pressure. The peridium is double-layered, with typically separated white layers. The spores possess a pronounced groove at the midpoint, resembling two opposed hemispherical spores. The capillitium contains fewer lime nodes.

Type: China, Sichuan Province, Mianyang City, Pingwu County, Hongyan Forest Farm, on the rotten branches and leaves, 21 July 2013, B. Zhang (HMJAU M20025, holotype).

Description: Sporocarps, sessile, gregarious, dense, often mutual extrusion deformation, hemispherical to spherical, (0.4–) 0.5–0.7 (–0.8) mm in diameter. Peridium two-layered, the outer layer calcareous, white, the inner layer separated from the outer layer, membranous, colourless and transparent. Columella present, white, hemispherical. Hypothallus white. Capillitium dense, brown, slender, winding, branched and connected, with many swelling knots, dark brown, lime nodes yellow, large, very less. Spores dark in mass, brown by TL, (11.5–) 12–13 (–14) µm in diameter, some warts connect to form a ridge, spores with a deep groove in the middle, resembling two adjoined hemispherical spores, with sparse warts and ridge by SEM. Plasmodium unknown.

Habitat: On the rotten branches and leaves.

Distribution in China: Sichuan Province.

Distribution in the world: China.

Additional materials examined: China, Sichuan Province, Mianyang City, Pingwu County, Hongyan Forest Farm, on the rotten branches and leaves, 21 July 2013, B. Zhang (HMJAU M20062, HMJAU M20063, HMJAU M20110, HMJAU M20111, HMJAU M20112).

Notes: The most distinguishing feature of this species is the groove at the centre of the spore, which creates the appearance of two adjoined hemispherical spores. Morphologically, *Diderma crustaceum* Peck is similar to *N. pseudobisporum* in terms of sporocarp colour, spore size, and columella colour. However, *N. pseudobisporum* can be distinguished from *D. crustaceum* by several features: *D. crustaceum* has a large, clavate columella and densely warted spores, whereas *N. pseudobisporum* possesses a smaller, hemispherical or flat pulvinate columella, capillitium with fewer lime nodes, and spores with sparsely distributed warts, with some smooth areas lacking warts. Phylogenetically, *N. pseudobisporum* forms a distinct branch with high support values (99.8/1) (Figure 1), and its morphological features set it apart from all currently reported species.

Neodiderma verrucocapillitium X.F. Li, B. Zhang & Y. Li, sp. nov. Figure 4

MycoBank: MB 852948.

Etymology: The epithet "*verrucocapillitium*" refers to the capillitium with verrucose.

Diagnosis: Sporocarps are densely packed and frequently exhibit deformation from mutual extrusion, ranging from greyish-white to white in colour. The peridium consists of two layers: an outer calcareous layer closely united with a membranous inner layer. The capillitium is dense, featuring numerous dark, thickened nodules that are spindle-shaped or

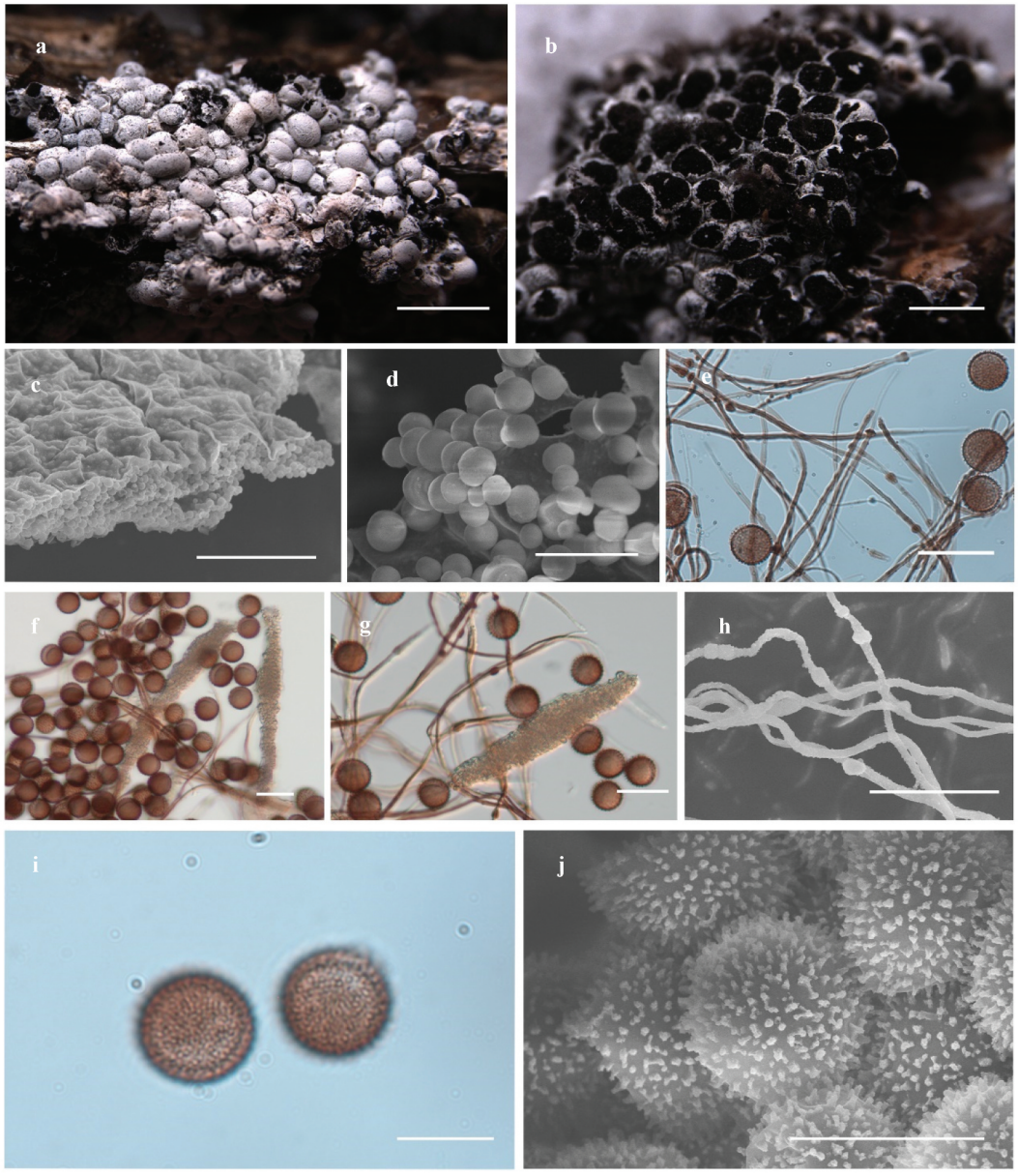

Figure 3. Habitat and microstructure of *Neodiderma pseudobisporum* (HMJAU M20025 holotype). (a, b) Sporocarps. (c) Two-layered peridium by SEM. (d) Limestone on the outer surface of the peridium. (e) Capillitium and spores by TL. (f, g) part of capillitium with swelling and lime nodes by TL. (h) Capillitium with swelling by SEM. (i) Spores by TL. (j) Spores marked with warts by SEM. Scale bars: a = 2 mm; b = 1 mm; c = 30 µm; d = 5 µm; e – h = 20 µm; i, j = 10 µm.

subglobose, along with yellow, spindle-shaped lime nodes. The spore mass is dark brown.

Type: China, Heilongjiang Province, Heihe City, Huma County, on the rotten leaves, 17 August 2022, X.F. Li (HMJAU M20039, holotype).

Description: Sporocarps, gregarious, sessile, white or pale-white, spherical or hemispherical, stacking, often mutual extrusion deformation, (0.65–) 0.71–0.89 (–0.95) mm in diameter. Peridium double-layered, thin, the outer layer calcareous, composed of a tightly packed layer of calcareous lime granules, white, the inner layer membranous, colourless, often tightly attached to the outer layer. Columella presence, hemispherical protrusion at the base, calcareous, light yellowish-brown. Hypothallus membranous, colourless and transparent, sometimes calcareous, white, connected into slices. Capillitium dense, abundant, brown, colourless at the end, dark thickened and spindle or subglobose shaped nodules, with yellow and spindle lime nodes. Spore dark brown in mass, reddish brown by TL, 8–9.5 (–10) µm in diameter, with sparse spiny. Plasmodium unknown.

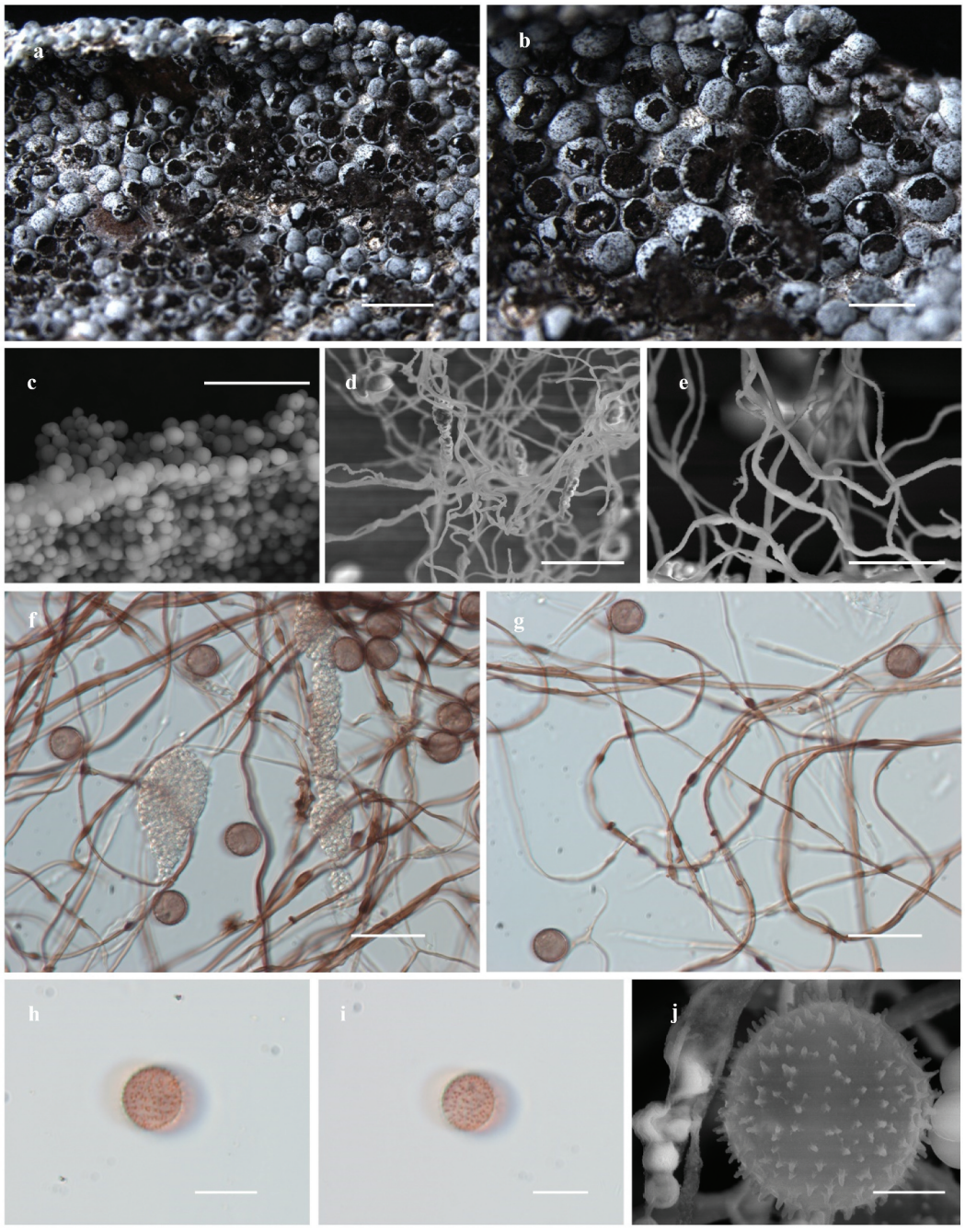

Figure 4. Habitat and microstructure of *Neodiderma verrucocapillitium* (HMJAU M20039 holotype). (a, b) Sporocarps. (c) Two-layered peridium by SEM. (d) Capillitium and lime nodes by SEM. (e) Capillitium by SEM. (f, g) Capillitium, spores and lime nodes by TL. (h–j) Spores by TL and SEM. Scale bars: a = 2 mm; b = 1 mm; c, e, h, i = 10 µm; d, f, g = 20 µm; j = 2 µm.

Habitat: On the rotten leaves.

Distribution in China: Heilongjiang Province.

Distribution in the world: China.

Additional specimens examined: China, Heilongjiang Province, Heihe City, Huma County, on the rotten leaves, 17 August 2022, X.F. Li (HMJAU M20040, HMJAU M20041).

Notes: *Neodiderma verrucocapillitium* is characterised by its white or grey sporocarp, two-layered peridium, hypothallus connected in slices, dense brown capillitium, dark, thickened, spindle- or subglobose-shaped nodules, and yellow, spindle-shaped lime nodes. Morphologically, it is highly similar to *Diderma alpinum*, as both exhibit white, dense sporocarps, a white hypothallus, and

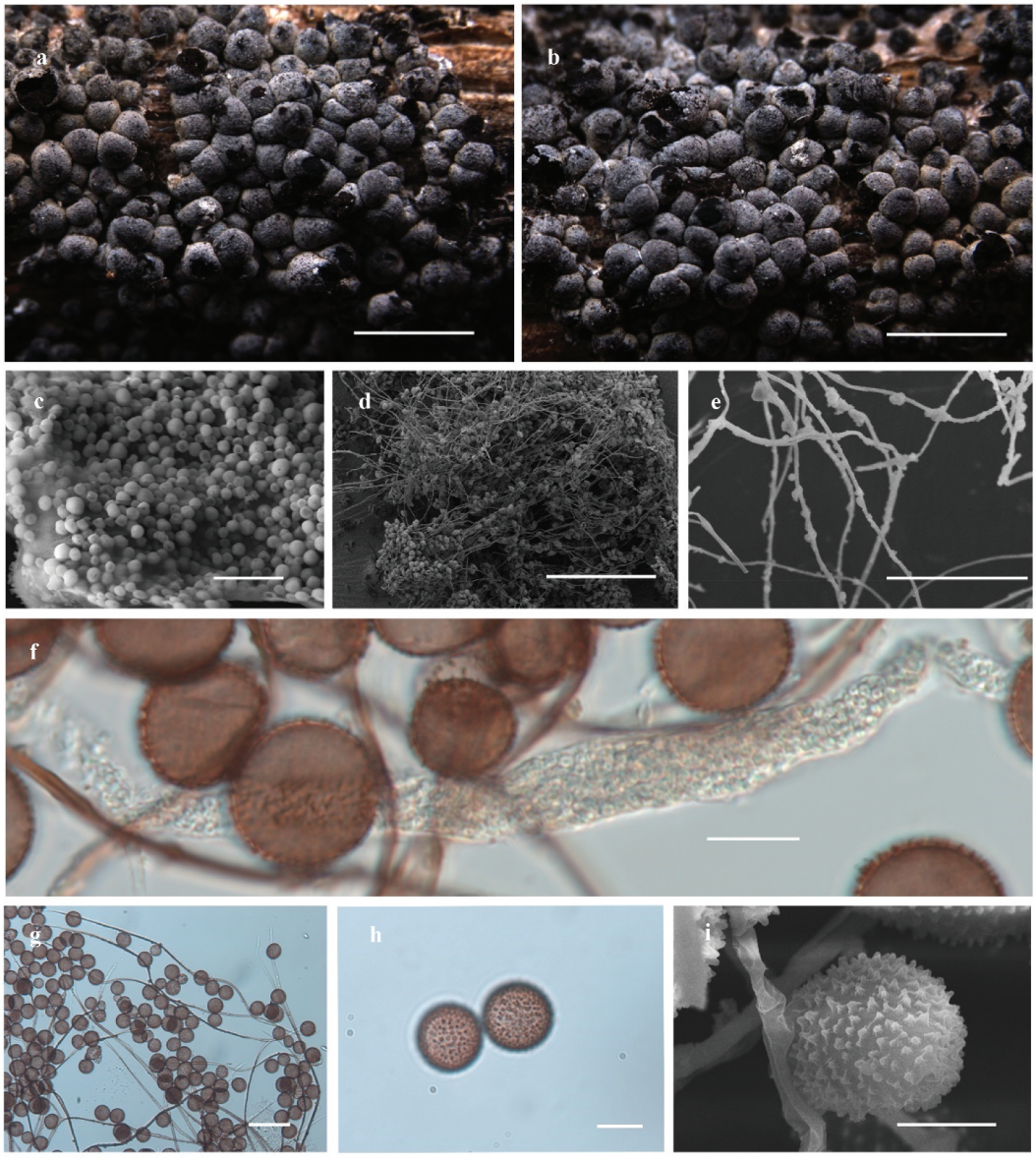

Figure 5. Habitat and microstructure of *Neodiderma rigidocapillitium* (HMJAU M20023 holotype). (a, b) Sporocarps. (c) Two-layered peridium by SEM. (d) Capillitium and some spores by SEM. (e) Capillitium with swellings and nodules by SEM. (f) Lime nodes and spores by TL. (g) Capillitium and some spores by TL. (h, i) Spores with spinulose and ridge by TL and SEM. Scale bars: a, b = 2 mm; c = 5 µm; d = 200 µm; e = 40 µm; f = 10 µm; g = 40 µm; h = 10 µm; i = 5 µm.

capillitium with dark, thickened, spindle- or subglobose-shaped nodules. However, *N. verrucocapillitium* differs from *D. alpinum* in having a hemispherical columella at the base, tighter attachment between the two peridium layers, fewer lime nodes in the capillitium, and smaller spores. Phylogenetically, our analysis indicates that *N. verrucocapillitium* forms a distinct branch with high support (98/0.99), clearly showing a close relationship with *N. rigidocapillitium* (Figure 1). Despite this relationship, significant morphological differences exist: *N. verrucocapillitium* has smaller spores [8–9.5 (–10) µm] with sparser spines, whereas *N. rigidocapillitium* has larger spores [(11.5–) 12–15 (–16) µm] with denser spines. These combined morphological and phylogenetic findings support our identification of *N. verrucocapillitium* as a novel species.

Neodiderma rigidocapillitium X.F. Li, B. Zhang & Y. Li, sp. nov. Figure 5

MycoBank: MB 852949.

Etymology: The epithet "*rigidocapillitium*" refers to the hard and inflexible capillitium of this species.

Diagnosis: Sporocarps are densely crowded, exhibiting a greyish-black to greyish-white

colouration. The peridium is two-layered, with a rough white outer layer tightly adhered to a membranous inner layer. The capillitium is hard and straight, with dark swellings and nodules, and contains fewer lime nodes. The spore mass is dark brown.

Type: China, Sichuan Province, Mianyang City, Pingwu County, Hongyan Forest Farm, on the dead branches, 21 July 2013, B. Zhang (HMJAU M20023, holotype).

Description: Sporocarps, gregarious, dense, sessile, hemispherical, often deformed due to mutual compression, greyish black to greyish white, halo at the base, (0.6–) 0.63–0.82 (–0.85) mm in diameter. Peridium two-layered, the outer layer calcareous, white, grey, easy to fall off, the inner membranous, iridescent. Columella present, conspicuous, slightly convex, cushion, white or cream yellow, with limy, uneven. Hypothallus present, white. Capillitium brown, hard and straight, with dark swellings and nodules, light colour at both ends, lime nodes yellow, large, very less. Spores dark brown in mass, light brown by TL, (11.5–) 12–15 (–16) µm in diameter, with shortly spiny, sometimes joining into ridges and smooth in some areas. Plasmodium unknown.

Habitat: On the dead branches.

Distribution in China: Sichuan Province.

Distribution in the world: China.

Additional specimens examined: China, Sichuan Province, Mianyang City, Pingwu County, Hongyan Forest Farm, on the dead branches, 21 July 2013, B. Zhang (HMJAU M20118, HMJAU M20119).

Notes: *Neodiderma rigidocapillitium* shares morphological similarities with *N. spumarioides*, as both species have white sporocarps with sessile, two-layered peridia (the outer layer being calcareous and the inner layer membranous), white hypothalli, and spinulose spores. However, *N. rigidocapillitium* differs by having capillitium with bulbous enlargements, whereas *N. spumarioides* rarely shows branching and has smaller thickenings. Though the two species have similar spore shape and ornamentation, *N. rigidocapillitium* has larger spores [(11.5–) 12–15 (–16) µm] compared to *N. spumarioides* (9–10 µm) and exhibits a denser spiny texture. Phylogenetic analysis based on nSSU, *EF-1α*, and *COI* sequences shows that *N. rigidocapillitium* is closely related to *N. verrucocapillitium*, forming a distinct branch with strong support (UBS = 98, PP = 0.99), although the two species exhibit clear morphological differences, particularly in spore size and structure. These findings, combining both morphological and phylogenetic evidence, justify the identification of *N. rigidocapillitium* as a new species.

Neodiderma rufum X.F. Li, B. Zhang & Y. Li, sp. nov. Figure 6

MycoBank: MB 852950.

Etymology: The epithet "*rufum*" refers to the red-brown and dark-brown peridium of this species.

Diagnosis: The sporocarps are smooth, with a dark brown or reddish-brown colouration. The peridium is double-layered and brittle, with the outer layer containing calcareous particles tightly adhered to the light brown inner layer. The columella is flat and pulvinate in shape. The capillitium contains fewer lime nodes, and the spores are dark.

Type: China, Sichuan Province, Liangshan Yi Autonomous Prefecture, Mianning County, on the rotten leaves, 12 July 2013, B. Zhang (HMJAU 60242, holotype).

Description: Sporocarps, sessile, scattered, hemispherical, smooth, (0.3–) 0.32–0.77 (–0.8) mm in diameter, dark brown or reddish brown. Peridium two-layered, the outer layer calcareous, more brittle, smooth, and the inner layer membranous, red-brown, tightly fused with the outer calcareous, glossy. Hypothallus absent. Columella presence, calcareous protuberance, flat pulvinate, and rusty brown or yellowish-brown. Capillitium slender filamentous, rough, brown, branching and connecting, lime nodes yellow, large, very less. Spores dark in mass, tawny by TL, (8.5–) 9–10 µm in diameter, ornamented with densely warts, the groups of wartlets appear rather indistinct. Plasmodium unknown.

Habitat: On the rotten leaves.

Distribution in China: Sichuan Province.

Distribution in the world: China.

Notes: The primary characteristic of *Neodiderma rufum* is the dark brown or reddish-brown sporocarp, featuring a smooth, calcareous peridium. *Neodiderma ochraceum* shares similarities with *N. rufum* in sporotheca shape, spore size, and the presence of a two-layered peridium. However, *N. rufum* is distinguished by a developed, flat pulvinate columella, spores with densely distributed warts, and a tendency to form clusters. In contrast, *N. ochraceum* has an indistinct or absent columella, and its spores are minutely

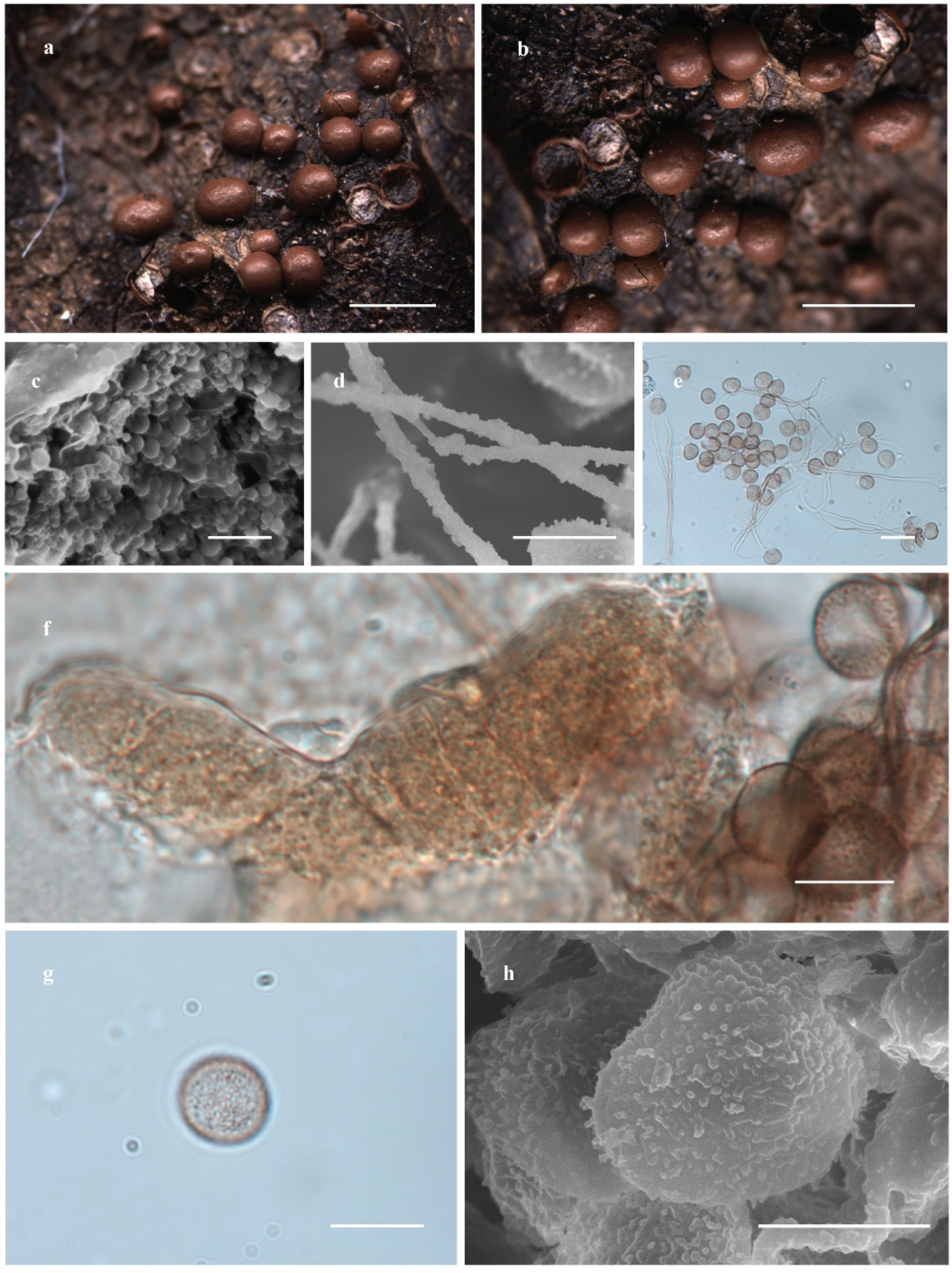

Figure 6. Habitat and microstructure of *Neodiderma rufum* (HMJAU 60242 holotype). (a) Sporocarps. (b) Columella. (c) Two-layered peridium by SEM. (d) Capillitium by SEM. (e) Capillitium and spores by TL. (f) Lime nodes by TL. (g) Spores by TL. (h) Spores with warts by SEM. Scale bars: a, b = 1 mm; c = 1 µm; d = 5 µm; e = 20 µm; f, g = 10 µm; h = 5 µm.

spinulose. From a phylogenetic perspective, our specimen (HMJAU 60242) forms a monophyletic clade with strong support (UBS = 95.2, PP = 1) and is closely related to *N. ochraceum* (formerly *Diderma ochraceum*) in the three-gene phylogenetic tree (Figure 1). Although the status of *N. ochraceum* remains uncertain due to insufficient data, our analysis groups *N. rufum* with other species in the genus *Neodiderma* into a large branch (Figure 1). Therefore, both the morphological and phylogenetic analyses strongly support our identification of *N. rufum* as a new species.

Neodiderma spumarioides (Fr. & Palmquist) X.F. Li, B. Zhang & Y. Li, comb. nov. Figure 7

MycoBank: MB 852951.

Basionym. *Diderma spumarioides* (Fr. & Palmquist) Fr., Syst. mycol. 3(1):104, 1829.

Neotype: Indiana, Clarck Co., on rotten leaves, Aug. 1938, Gray (NY 8712, neotype).

Description: Sporocarps, gregarious, dense, spherical to subglobose, rough, white or pale grey, often distorted by mutual pressure, (0.35–) 0.4–0.8 (–0.85) mm in diameter. Sessile, sporocarps buried in a white to ivory expanded hypothallus. Columella inconspicuous, rounded and convex, pulvinate or hemispherical, grey-white. Peridium two-layered, the outer layer

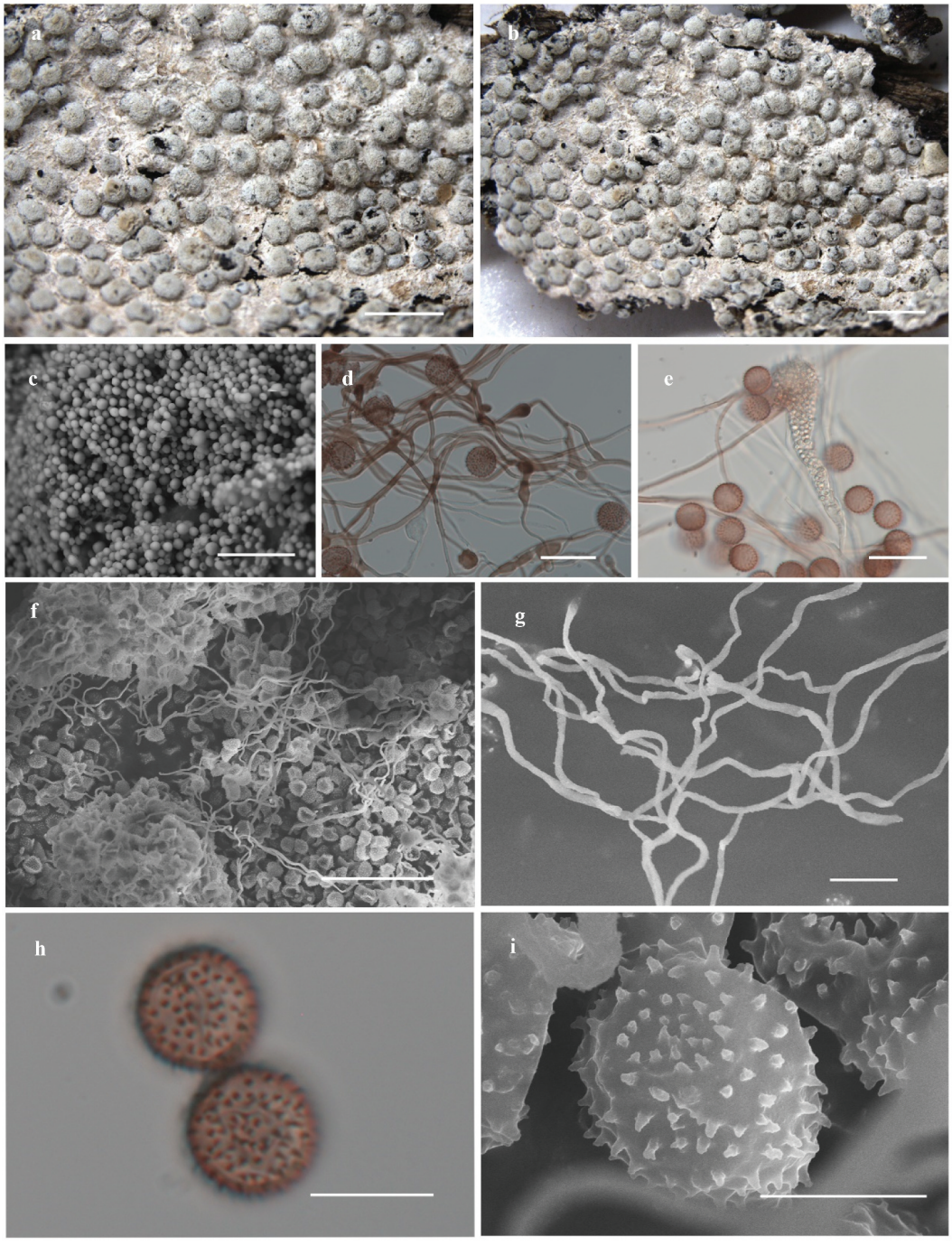

Figure 7. Habitat and microstructure of *Neodiderma spumarioides* (HMJAU M20028). (a, b) Sporocarps. (c) Two-layered peridium by SEM. (d) Capillitium and spores by TL. (e) Capillitium, spores and lime nodes by TL. (f, g) Capillitium by SEM. (h, i) Spores with sparse spinules by TL and SEM. Scale bars: a, b = 2 mm; c, g, h = 10 µm; d, e = 20 µm; f = 50 µm; i = 5 µm.

calcareous, rough, thick, grey, the inner layer membranous, dark grey, orange-yellow at the base, tightly adhered with the outer layer. Hypothallus conspicuous, white, calcareous. Capillitium intertwined, curved, brown, very rarely branched, with small thickenings, lime nodes yellow, very less. Spores dark brown in mass, fawn-coloured by TL, with sparse spinules, (8.5–) 9–10 (–11) µm in diameter. Plasmodium unknown.

Habitat: On the rotten woods.

Distribution in China: Beijing City, Gansu Province, Hebei Province, Heilongjiang Province, Henan Province, Hunan Province, Inner Mongolia Autonomous Region, Jiangsu Province, Jilin Province, Qinghai Province, Taiwan Province, and Yunnan Province.

Distribution in the world: Algeria, Australia, Austria, Bahamas, Belgium, Bermuda, Canada, Chile, China, Denmark, Finland, France, Germany, Guatemala, India, Indonesia, Italy, Japan, Kazakhstan, Martinique, Mexico, Morocco, Nepal, New Zealand, Norway, Panama, Peru, Poland, Portugal, Puerto Rico, Russia, Spain, Sweden, the United States, United Kingdom, Uruguay, Uzbekistan, and Venezuela.

Specimens examined: China, Jilin Province, Baishan, Fusong County, Lushuihe Town, on the rotten woods, 22 July 2012, B. Zhang (HMJAU M20028); China, Jilin Province, Baishan, Fusong County, Lushuihe Town, on the rotten woods, 4 October 2001, H.Z. Liu & Tolgor (HMJAU 11078).

Notes: *Neodiderma spumarioides* shares morphological similarities with *Diderma cinereum* in its white and grey sporocarp, irregular dehiscence, white columella, brown capillitium, and similar spore sizes. However, several distinguishing features set *N. spumarioides* apart: it has a developed hypothallus, capillitium with swollen nodules, and a distortion caused by mutual pressure. Additionally, *N. spumarioides* has a two-layered peridium that is tightly adhered, giving the appearance of a single layer, whereas *D. cinereum* has a single, thin peridium layer. The presence of dispersed spinules also differentiates *N. spumarioides* at the microstructural level. From a phylogenetic standpoint, our specimens (HMJAU M20028 and HMJAU 11078) and *N. spumarioides* (MCCNNU2749) were grouped into a monophyletic clade with strong support (UBS = 98.3, PP = 1) (Figure 1). Thus, the identification of *N. spumarioides* is supported by both morphological and phylogenetic analyses.

Key to the species of genera *Physarum* present in this study

1. Peridium single layer.....3
2. Sessile, spores have large size (11–12 µm) .....*Physarum neoovoideum*
2. Short-stalk, spores have small size (9–11 µm) .....*Physarum leucophaeum*
3. Sporocarps yellow or yellow-green.....4
3. Sporocarps white or greyish-white, black.....5
4. Sporocarps usually nodding.....6
4. Sporocarps erect.....7
5. Sporocarps, stipitate.....8
5. Sporocarps or short plasmodiocarps, sessile.....9
6. Spores size >9 µm, with spiny, less lime nodes .....*Physarum subviride*
6. Spores size <9 µm, with warts, more lime nodes .....*Physarum viride*
7. Sporocarps bright yellow or orange, spores size >9 µm, with spiny, capillitium hard and straight, lime nodes light yellow .....*Physarum rigidum*
7. Sporocarps light yellow, spores size <9 µm, with warts, capillitium with orange lime nodes .....*Physarum psittacinum*
8. Stalk creamy-white or light-yellow, calcareous, spores 8–9 µm in diam....*Physarum guangxiense*
8. Stalk white to light ochraceous at apex, becoming fuliginous brown or black towards the base, without calcareous, spores (8.5) 9–10 µm in diam.....*Physarum album*
9. Spores size >9 µm, lime nodes small circular or elongated.....*Physarum jilinense*
9. Spores size <9 µm, lime nodes polygonal.....10
10. Sporocarps white, peridium covered with a layer of white calcareous scales on the surface .....*Physarum biyangense*
10. Sporocarps black with a bluish-purple halo, peridium smooth, without calcareous particles.....*Physarum nigritum*

Physarum guangxiense X.F. Li, B. Zhang & Y. Li, sp. nov. Figure 8

MycoBank: 854656.

Etymology: The epithet "*guangxiense*" refers to Guangxi, the location of the holotype.

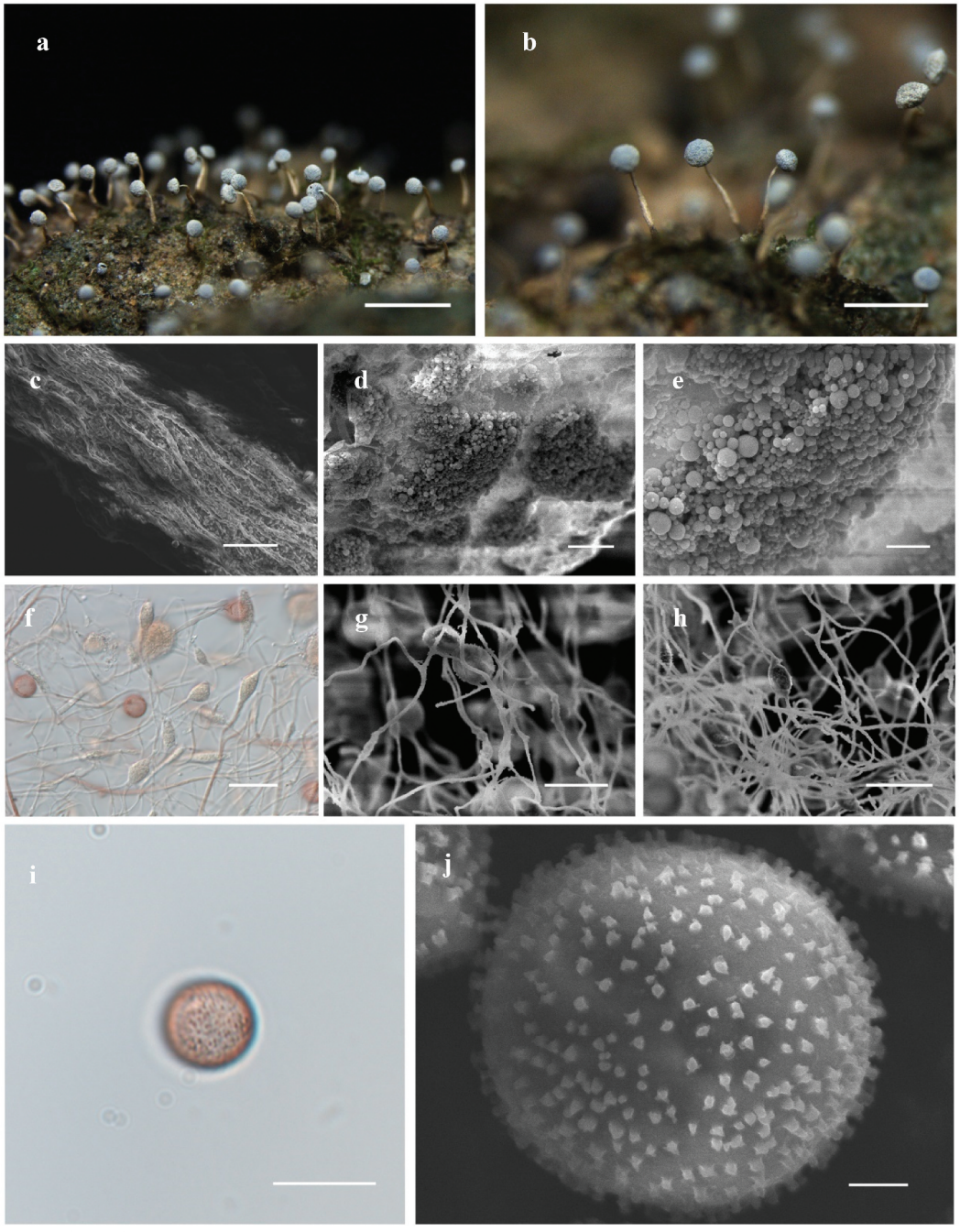

Figure 8. Habitat and microstructure of *Physarum guangxiense* (HMJAU M20344). (a, b) Sporocarps. (c) Stalk by SEM. (d) Single layer peridium by SEM. (e) Limestone on the outer surface of the peridium. (f–h) Capillitium and lime nodes by TL and SEM. (i, j) Spores by TL and SEM. Scale bars: a = 2 mm; b = 1 mm; c, f = 20 µm; d = 5 µm; e = 2 µm; g, h, i = 10 µm; j = 1 µm.

Diagnosis: The sporocarps are subglobose with stipitate, often nodding. The stalk is slender and light yellow. The peridium is wrinkled and covered with white lime globules. Columella is absent. The capillitium is connected to white, fusiform lime nodes. The spore mass is dark.

Type: China, Guangxi Zhuang Autonomous Region, Yachang County, on the rotten woods, 14 July 2017, B. Zhang (HMJAU M20344, holotype).

Description: Sporocarps, stipitate, gregarious, nodding, sporotheca white or greyish-white, (0.3–) 0.33–0.48 (–0.5) mm in diameter,

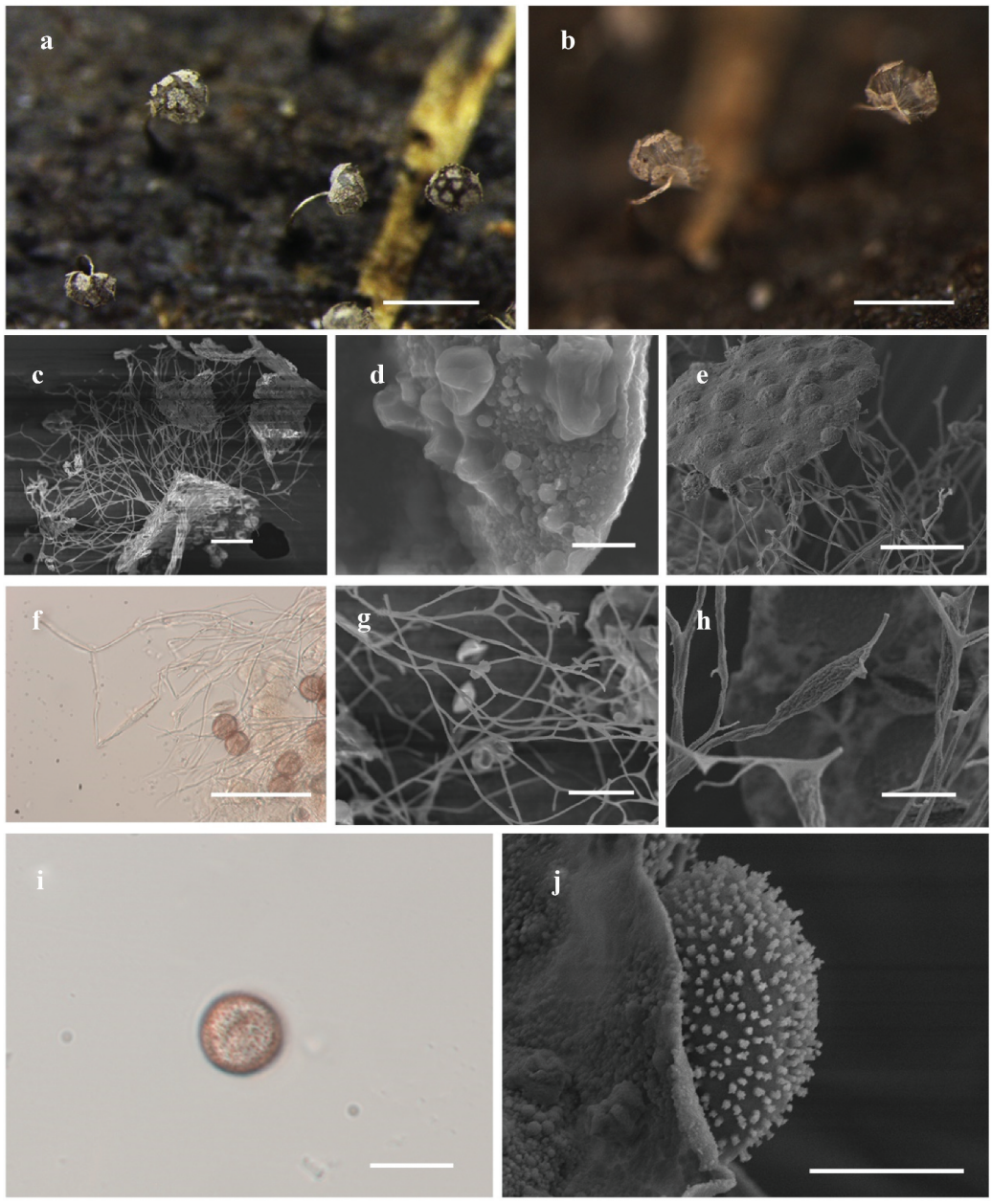

Figure 9. Habitat and microstructure of *Physarum subviride* (HMJAU M10138). (a, b) Sporocarps. (c) Sporothecae by SEM. (d) Peridium by SEM. (e) Capillitium and peridium by SEM. (f–h) Capillitium and lime nodes by TL and SEM. (i, j) Spores by TL and SEM. Scale bars: a, b = 500 μm; c = 40 μm; d = 2 μm; e, f = 40 μm; g = 20 μm; h, i = 10 μm; j = 5 μm.

(0.65–) 0.69–1.04 (–1.1) mm in height. Stalk slender, gradually tapering upwards, white, creamy-white or light yellow, calcareous, (0.65–) 0.67–0.87 (–0.9) mm in length. Peridium single layer, membranous, with a layer of white and thick lime granules on the surface, iridescent when without limy. Columella absent. Hypothallus inconspicuous. Capillitium dense mesh, colourless, lime nodes usually elongate, 11–30 × 3–6 μm, fusiform, white, less, bifurcated. Spores dark in mass, brown by TL, (7.5–) 8–9 μm in diameter, with warts. Plasmodium unknown.

Habitat: On the rotten woods.

Distribution in China: Guangxi Zhuang Autonomous Region.

Distribution in the world: China.

Additional specimens examined: Guangxi Zhuang Autonomous Region, Yachang County, on the rotten woods, 14 July 2017, B. Zhang (HMJAU M20345).

Notes: *Physarum guangxiense* exhibits morphological similarities to *P. album* (Bull.) Chevall. and *P. stellatum* in its white or greyish-white sporotheca, slender stalk, calcareous single-layer structure, white lime nodes, and similar spore sizes. Despite these similarities, clear distinctions exist. *P. guangxiense* has a white, grey-white, or light-yellow stalk that contains calcium but lacks dark matter, and its peridium surface is covered with a thick layer of calcareous scales. In contrast, *P. album* has a black or dark brown stalk base, with the upper portion ranging from white to light ochre, and contains dark substances in its stalk. Furthermore, *P. album* has a peridium covered with small white lime particles. When compared to *P. stellatum*, *P. guangxiense* shows differences in dehiscence; it is not easily dehiscent and has fusiform lime nodes, whereas *P. stellatum* often exhibits peridial dehiscence upon maturity and features oval or nearly fusiform lime nodes. From a phylogenetic perspective, our specimen (HMJAU M20344) is related to *P. leucophaeum*, *P. stellatum*, *P. album*, and *P. viride*. However, the genetic distance between *P. guangxiense* and these species is relatively large, resulting in its placement on a separate branch (Figure 1).

Physarum subviride X.F. Li, B. Zhang & Y. Li, sp. nov. Figure 9

MycoBank: 854657.

Etymology: The epithet "*subviride*" refers to overall characteristics are similar with the *Physarum viride*.

Diagnosis: This species closely resembles *P. viride*, with a slender stalk and white-yellow sporotheca, but its spores are larger than those of *P. viride*. The capillitium is connected to fewer light-yellow lime nodes.

Type: China, Jiangxi Province, Fuzhou City, Junfeng Mountain, on the rotten woods, 19 June 2013, B. Zhang (HMJAU M10138, holotype).

Description: Sporocarps, erect, usually nodding, gregarious, sporotheca yellowish-green, spherical or hemispherical, often slightly umbilicate, 0.3–0.4 (–0.5) mm in diameter, (0.5–) 0.6–0.9 (–1.0) mm in height. Stalk slender, subulate, curved at apex, (0.4–) 0.5–0.7 (–0.8) mm in length, white at apex, becoming fuliginous brown or black towards the base, containing dark substances. Columella absent. Hypothallus membranous, colourless and transparent. Peridium membranous, thin, covered at the top with a calcareous layer, scaly, white, iridescent, connected to capillitium. Dehiscent irregular. Capillitium thin, dense, radiantly extending from the base of the sporocarp, persistent, colourless, brown by TL, the lime nodes less, light yellow, small and fusiform. Spores dark brown in mass, brown under TL, (9–) 10–11 (12) µm in diameter, with warts. Plasmodium unknown.

Habitat: On the rotten woods.

Distribution in China: Jiangxi Province.

Distribution in the world: China.

Additional specimens examined: China, Jiangxi Province, Fuzhou City, Junfeng Mountain, on the rotten woods, 19 June 2013, B. Zhang (HMJAU M21304, HMJAU M21305).

Notes: *Physarum subviride* is characterised by its yellowish-green, nodding, and oblate sporotheca, with a slender stalk and an absent columella. The lime nodes are fusiform and sparse, and the spores are warty. Although *P. subviride* shares some similarities with *P. album* and *P. viride* in terms of sporotheca shape and colour, there are distinct differences. *P. album* and *P. viride* both have smaller spores (7–10 µm) and longer stalks (0.9–2.0 mm), whereas *P. subviride* has larger spores [(9–) 10–11 (–12) µm] and shorter stalks [(0.4–) 0.5–0.7 (–0.8) mm], with lime nodes that are rarely observed. Phylogenetic analysis based on nSSU, *EF-1α*, and *COI* genes places our specimen (HMJAU M10138) in a monophyletic clade with *P. guangxiense* (HMJAU M20344) (Figure 2, UBS = 100, PP = 1), although the genetic distance between them is relatively significant. The genetic distance of *P. subviride* from *P. leucophaeum*, *P. stellatum*, *P. album*, and *P. viride* further establishes it as an independent branch. Despite the literature suggesting *P. viride* may be a complex species (García-Martín et al. 2023), the morphological and phylogenetic analyses support the identification of *P. subviride* as a distinct new species.

Physarum nigritum X.F. Li, B. Zhang & Y. Li, sp. nov. Figure 10

MycoBank: 854936.

Etymology: The epithet "*nigritum*" refers to the dark sporocarp of this species.

Diagnosis: This species has a dark sporocarp with a blue-purple halo and lacks calcareous particles on the surface of the peridium. The peridium is membranous, smooth, and has a halo. The capillitium is connected to large, white, angular lime nodes. The spore mass is dark brown.

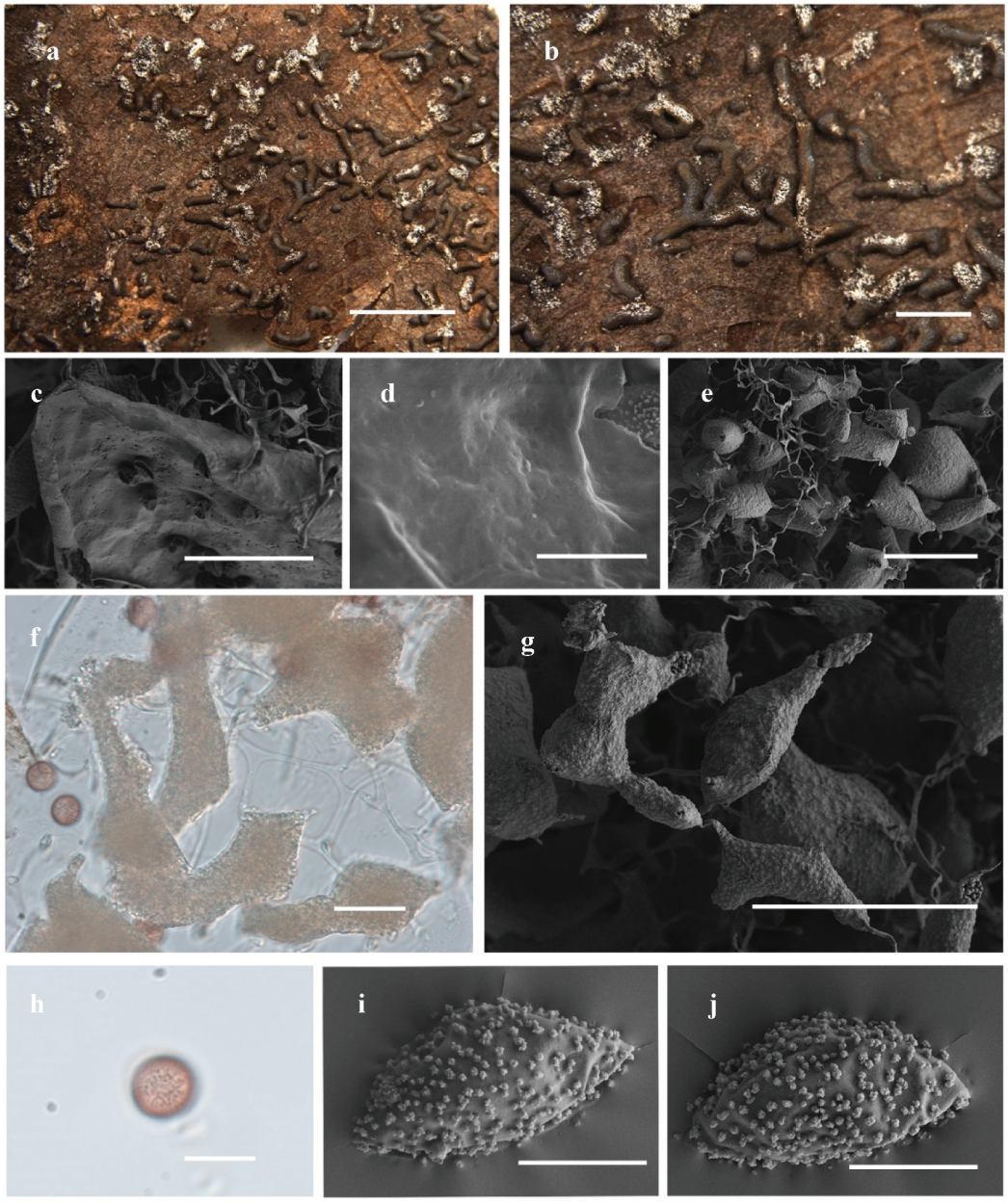

Figure 10. Habitat and microstructure of *Physarum nigritum* (HMJAU M21287). (a, b) Plasmodiocarps. (c, d) Peridium by sem. (e–g) Capillitium and lime nodes by TL and SEM. (h–j) Spores by TL and SEM. Scale bars: a = 5 mm; b = 2 mm; c = 40 µm; d = 5 µm; e, g = 50 µm; f = 20 µm; h = 10 µm; i, j = 4 µm.

Type: China, Anhui Province, Mazongling National Nature Reserve, on the rotten leaves, 14 June 2023, Y.L Tuo (HMJAU M21287, holotype).

Description: Sporocarps or plasmodiocarps, sessile, sporotheca elliptical or subglobose, gregarious, black, with a bluish-purple halo, (0.3–) 0.34–0.57 (–0.6) mm in diameter, plasmodiocarp straight or forked, curved, (0.55–) 0.59–3.85 (–3.9) mm in length, (0.5–) 0.25–0.36 (–0.4) mm in width. Peridium single layer, membranous, smooth, without calcareous particles, with blue purple halo, colourless under transmitted light, irregular dehiscent. Columella and hypothallus absent. Capillitium slender, colourless, and transparent, forming a dense net of hyaline threads with many white irregular lime nodes, 35–95 × 11–35 µm, with enlarged membranous enlargement. Spores dark brown in mass, light brown under TL, 8–9 (–9.5) µm in diameter, with warts. Plasmodium unknown.

Habitat: On the rotten leaves.

Distribution in China: Anhui Province, Henan Province.

Distribution in the world: China.

Additional specimens examined: China, Henan Province, Zhumadian City, Biyang County, Yansheng Botanical Garden, on the rotten leaves, 11 June 2023, B. Zhang (HMJAU M20277, HMJAU M20276, HMJAU M20279).

Notes: *Physarum nigritum* is primarily characterised by the dark colouration of its sporocarp, which features a distinct blue-purple halo, a single-layer peridium, and a surface devoid of calcareous particles. The species lacks a columella, and its lime nodes are white and irregular. Morphologically, *P. nigritum* is similar to *P. parvicalcareum*, as both species possess a dark sporocarp with a halo and a single-layer peridium. However, *P. nigritum* can be differentiated by its smaller spores (8–9 µm), larger lime nodes, and absence of a hypothallus, while *P. parvicalcareum* has larger spores (10–11 µm), smaller lime nodes, and a continuous hypothallus. From a phylogenetic perspective (Figure 1), our specimens of *P. nigritum* (HMJAU M20277, HMJAU M20276, HMJAU M20279, and HMJAU M21287) are related to *P. cinereum*, forming a separate branch. Despite this relationship, the genetic distance between the two species is significant, and their morphological characteristics differ notably. Thus, both the morphological and phylogenetic analyses support the identification of *P. nigritum* as a new species.

Physarum biyangense X.F. Li, B. Zhang & Y. Li, sp. nov. Figure 11

MycoBank: 854658.

Etymology: The epithet "*biyangense*" refers to Biyang County, the location of the holotype.

Diagnosis: The sporocarps or short plasmodiocarps have numerous calcareous scales on the surface, exhibiting a white colouration. The peridium is single-layered, membranous, and studded with rounded white limy scales. The capillitium is delicate and contains dense, angular lime nodes. The spores are smaller.

Type: China, Henan Province, Zhumadian City, Biyang County, Wanfeng Temple, on the rotten leaves, 12 June 2023, B. Zhang (HMJAU M20349, holotype).

Description: Sporocarps or short plasm odiocarps, gregarious or scattered, white, sessile, (0.45–) 0.5–2.27 (–2.3) mm in length, (0.28–) 0.31–0.4 (–0.5) mm in width. Peridium thin, membranous, covered with a layer of white calcareous scales on the surface, numerous, the sporotheca or synapsis is generally calcium free and dark on the base. Columella and hypothallus absent. Capillitium dense, colourless, and transparent, lime nodes numerous, white, polygonal, with enlarged membranous enlargement. Spores dark in mass, red-brown under TL, 7–8.5 (–9) µm in diameter, with warts. Plasmodium unknown.

Habitat: On the rotten leaves.

Distribution in China: Henan Province.

Distribution in the world: China.

Additional specimens examined: China, Henan Province, Zhumadian City, Biyang County, Wanfeng Temple, on the rotten leaves, 13 June 2023, B. Zhang (HMJAU M21306, HMJAU M21307).

Notes: *Physarum biyangense* shares similarities with *P. cinereum* and *P. vernum*, including its white or greyish-white sporotheca and the presence of white, polygonal lime nodes. However, *P. biyangense* can be distinguished from *P. cinereum* by its larger lime nodes and smaller spores (7–8.5 µm), compared to *P. cinereum*'s smaller lime nodes and larger spores (9–12 µm). Additionally, *P. vernum* has a thicker peridium and a rougher texture due to uneven limestone coverage, with larger spores (9–12 µm), differentiating it from *P. biyangense*. Table 3 provides a detailed comparison of these species. Our phylogenetic analysis (Figure 1) places *P. biyangense* (HMJAU M20349) and other related specimens in a distinct branch from *P. cinereum*, with significant genetic distance and morphological differences, supporting the identification of these as new species.

Physarum neoovoideum X.F. Li, B. Zhang & Y. Li, sp. nov. Figure 12

MycoBank: 854659.

Etymology: The epithet "*neoovoideum*" refers to subspherical or oval sporocarp of this species.

Diagnosis: The sporocarps are oval-shaped with numerous white calcareous particles on the surface of the peridium, which is rough. The outer layer is calcareous, thick, and pale white, while the inner layer is membranous and colourless. The capillitium is connected to large, numerous, angular lime nodes, which sometimes gather at the centre to form a pseudocolumella.

Type: China, Jilin Province, Changchun City, Jilin Agricultural University Campus, on the rotten leaves, 30 July 2018, B. Zhang (HMJAU M20294, holotype).

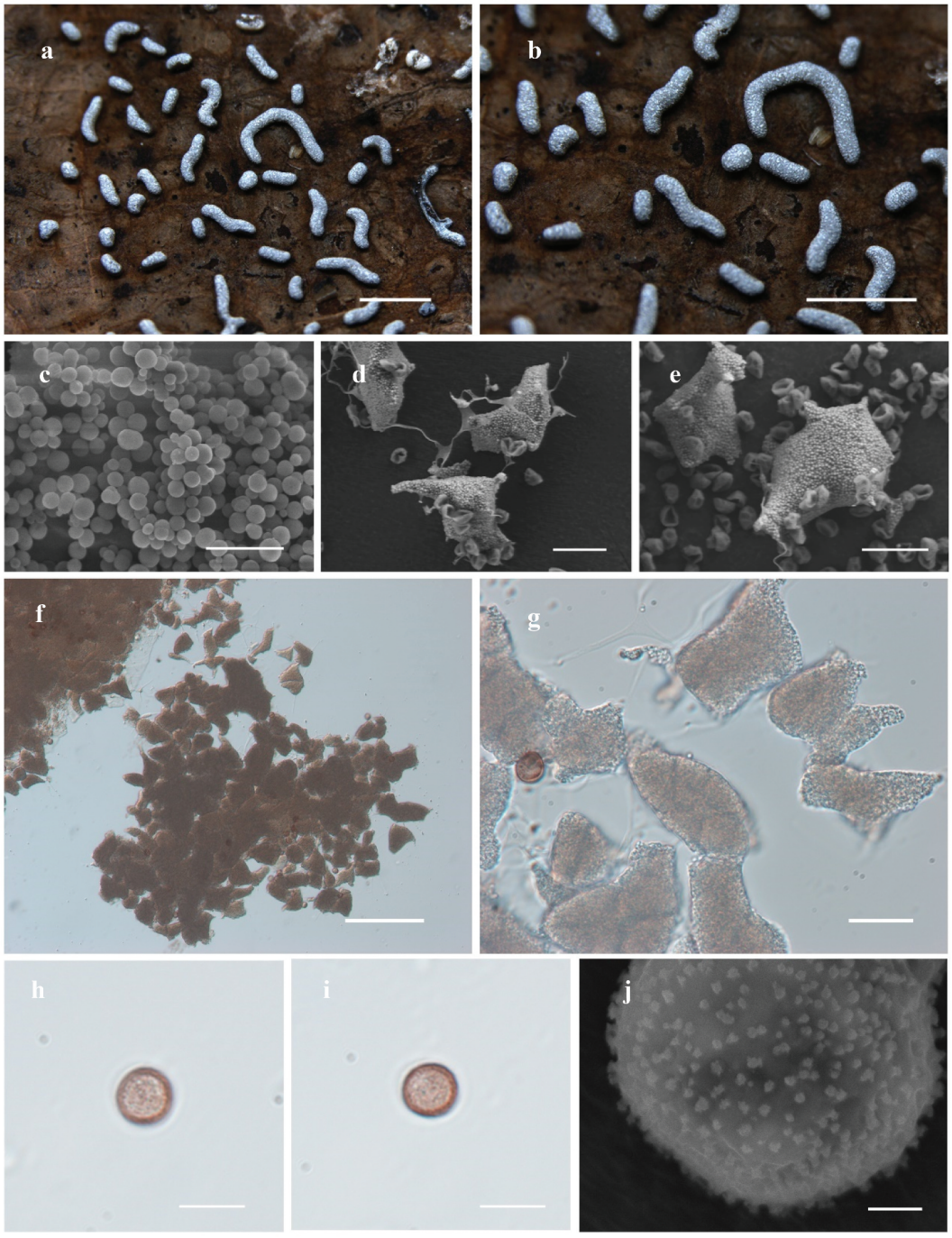

Figure 11. Habitat and microstructure of *Physarum biyangense* (HMJAU M20349). (a, b) Plasmodiocarps. (c) limestone on the peridium. (d, e) Capillitium and lime nodes by SEM. (f, g) Capillitium and lime nodes by TL. (h–j) Spores by TL and SEM. Scale bars: a, b = 2 mm; c = 4 μm; d, e, g = 20 μm; f = 100 μm; h, i = 10 μm; j = 1 μm.

Description: Sporocarps, sessile, gregarious, sometimes forming short-plasmodiocarps, twisted, grey white, (0.4–) 0.46–0.89 (–0.92) mm in length, (0.3–) 0.33–0.51 (–0.55) mm in width. Peridium two-layered, the outer layer calcareous, covered with white calcareous particles on the surface, white or greyish-white, rough, the inner layer membranous, adheres closely from the outer layer. Columella absent, lime nodes often form a pseudocolumella in the middle. Hypothallus inconspicuous. Capillitium dense, colourless, and transparent, the lime nodes numerous, white, large, and polygonal, with enlarged

Table 3. Comparison of morphological characteristics of *Physarum biyangense, Physarum neoovoideum*, *Physarum cinereum*, *Physarum vernum*.

Species name	Sporocarps	Peridium	Columella	Capillitium	Spores
P. biyangense	Sporocarps or short plasmodiocarps, white, sessile, (0.45–) 0.5–2.27 (−2.3) mm in length, (0.28–) 0.31–0.4 (−0.5) mm in width.	Peridium single, membranous, covered with a layer of white calcareous scales on the surface.	Absent.	Capillitium dense, lime nodes numerous, white, polygonal.	Spores with warts, 7–8.5(−9) µm in diameter.
P. neoovoideum	Sporocarps or short plasmodiocarps, sessile, grey white, (0.4–) 0.46–0.89 (−0.92) mm in length, (0.3–) 0.33–0.51 (−0.55) mm in width.	Peridium two-layered, the outer layer calcareous, the inner layer membranous, adheres closely from the outer layer.	Absent.	Capillitium dense, lime nodes numerous, white, large and polygonal.	Spores with warts, (10–)11–12 µm in diameter.
P. cinereum	Sporocarps to short plasmodiocarps, sessile, white or grey, or nearly limeless. 0.3–0.5 mm diameter.	Peridium single, thin, densely coated or flecked with lime.	Absent.	Capillitium dense, lime nodes angular.	Spores with warts, (7–) 9–12 µm in diameter.
P. vernum	Sporocarps or short plasmodiocarps, sessile, greyish white, (0.3–) 0.5–0.8 (−1) mm diameter.	Peridium single, membranous, usually densely covered with coarse, closely-set calcareous globules, rarely nearly limeless.	Absent.	Capillitium dense, lime nodes large, angular.	Spores with warts, (9–)10–12 µm in diameter.

membranous enlargement. Spores dark in mass, brown by TL, (10–) 11–12 µm in diameter, with warts. Plasmodium unknown.

Habitat: On the rotten leaves.

Distribution in China: Jilin Province.

Distribution in the world: China.

Additional specimens examined: China, Jilin Province, Changchun City, Jilin Agricultural University Campus, on the rotten leaves, 5 August 2018, B. Zhang (HMJAU M21308, HMJAU M21309).

Notes: *Physarum neoovoideum* is morphologically similar to *P. bryomacrocarpum* due to its sessile sporocarp and white, polygonal lime nodes. However, it differs from *P. bryomacrocarpum* by its white or grey-white peridium and smaller, spherical spores (11–12 µm) with warty textures, whereas *P. bryomacrocarpum* has a cream to brown peridium and larger, spiny spores (14.5–16 µm or 15–17.5 × 16.5–20 µm). Our phylogenetic analysis based on nSSU, *EF-1α*, and *COI* sequences places *P. neoovoideum* (HMJAU M20294) in a separate branch from *P. cinereum* (MA-Fungi 63822 and MA-Fungi 70925) and other related specimens, with significant genetic distance. This supports the identification of *P. neoovoideum* as a new species.

Physarum jilinense X.F. Li, B. Zhang & Y. Li, sp. nov. Figure 13

MycoBank: 854660.

Etymology: The epithet "*jilinense*" refers to Jilin, the location of the holotype.

Diagnosis: This species often grows on dry grass stems. The sporocarps are sessile, sometimes mingling with short plasmodiocarps. The peridium is single-layered, rough, wrinkled, and covered with a calcareous layer. The lime nodes connected by the capillitium are white, small, circular, elongated, or angular, and numerous, sometimes forming a pseudocolumella.

Type: China, Jilin Province, Changchun City, Jilin Agricultural University Campus, on the withered grass stem, 30 July 2018, B. Zhang (HMJAU M20367, holotype).

Description: Sporocarps or short plasmodiocarps, sessile, scattered, subglose or ellipsoidal, white or greyish-white, (0.55–) 0.59–1.26 (−1.3) mm in length, (0.35–) 0.39–0.58 (−0.6) mm in width. Peridium single layer, membranous, thin, covered with white calcareous scales on the surface, rough, wrinkled, colourless, and transparent when no calcium. Columella absent, sometimes forming pseudocolumella. Hypothallus inconspicuous. Capillitium dense, colourless, and transparent, the lime nodes numerous, white, small circular or elongated, sometimes larger polygonal, with enlarged membranous enlargement. Spores dark in mass, light brown by TL, subglobose, (9.5–) 10–11 µm in diameter, with warts. Plasmodium unknown.

Habitat: On the withered grass stem.

Distribution in China: Jilin Province.

Distribution in the world: China.

Additional specimens examined: China, Jilin Province, Changchun City, Jilin Agricultural University Campus, on the withered grass stem, 10 August 2018, B. Zhang (HMJAU M21310, HMJAU M21311).

Notes: *Physarum jilinense* shares several morphological similarities with *P. licheniforme* and

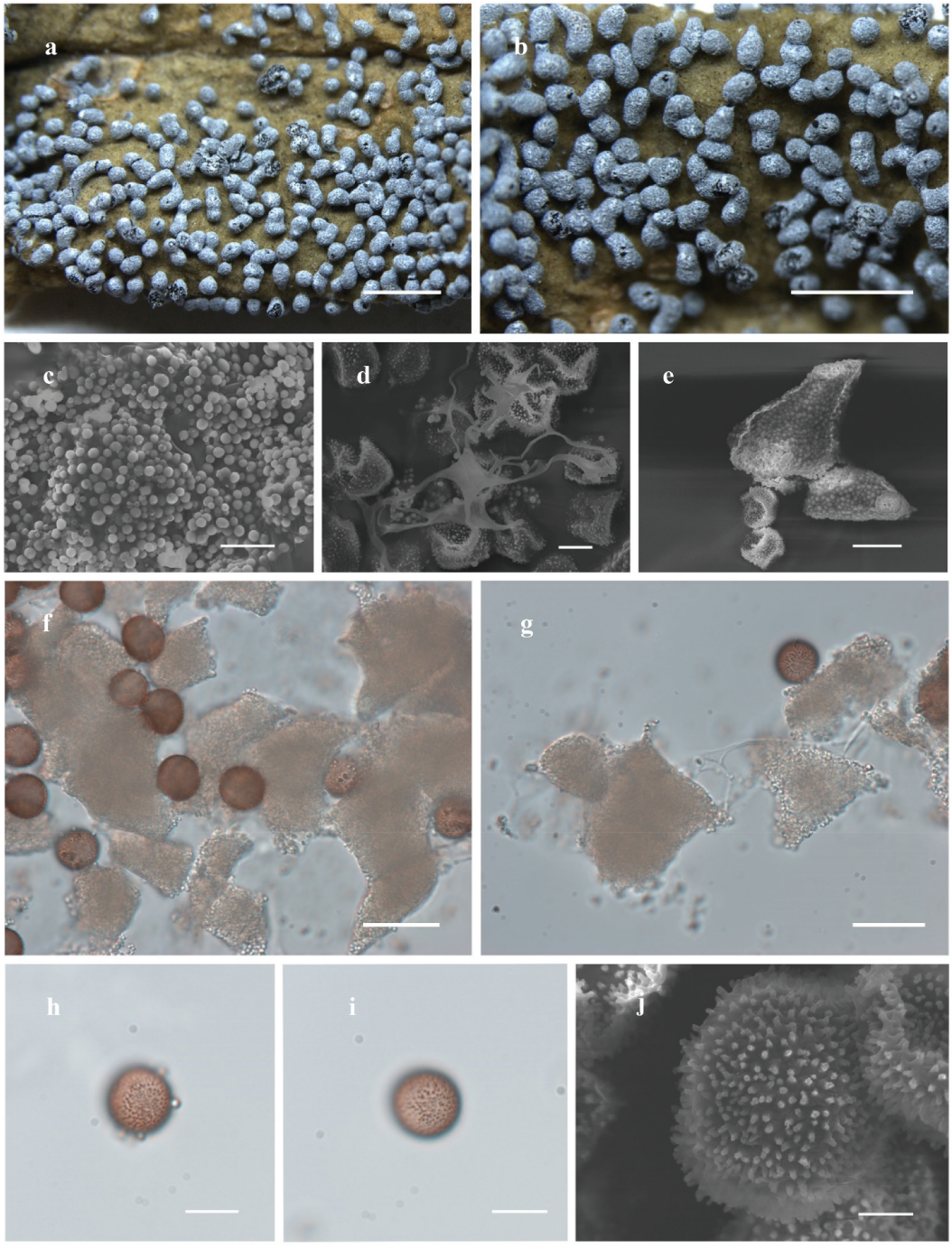

Figure 12. Habitat and microstructure of *Physarum neoovoideum* (HMJAU M20294). (a, b) Sporocarps. (c) Peridium by SEM. (d, e) Capillitium and lime nodes by SEM. (f, g) Capillitium and lime nodes by TL. (h–j) Spores by TL and SEM. Scale bars: a, b = 2 mm; c, d = 5 μm; e–i = 10 μm; j = 2 μm.

P. didermoides, such as light grey or greyblue-grey sporocarp, spherical or subglobose shape, white lime nodes, and the absence of a columella. However, *P. jilinense* can be distinguished from *P. licheniforme* by its smaller spores (10–11 μm) and its tendency to remain rarely dehiscent, while *P. licheniforme* often exhibits irregular dehiscence, with the base remaining as a cup. Additionally, compared to *P. didermoides*, *P. jilinense* has a single-layer peridium, whereas *P. didermoides* features a double-layered peridium and sometimes exhibits a white or reddish stalk. Phylogenetically (Figure 1), our specimen of *P. jilinense* (HMJAU M20367) and *P. didermoides* (MA-Fungi 71195 and MA-Fungi

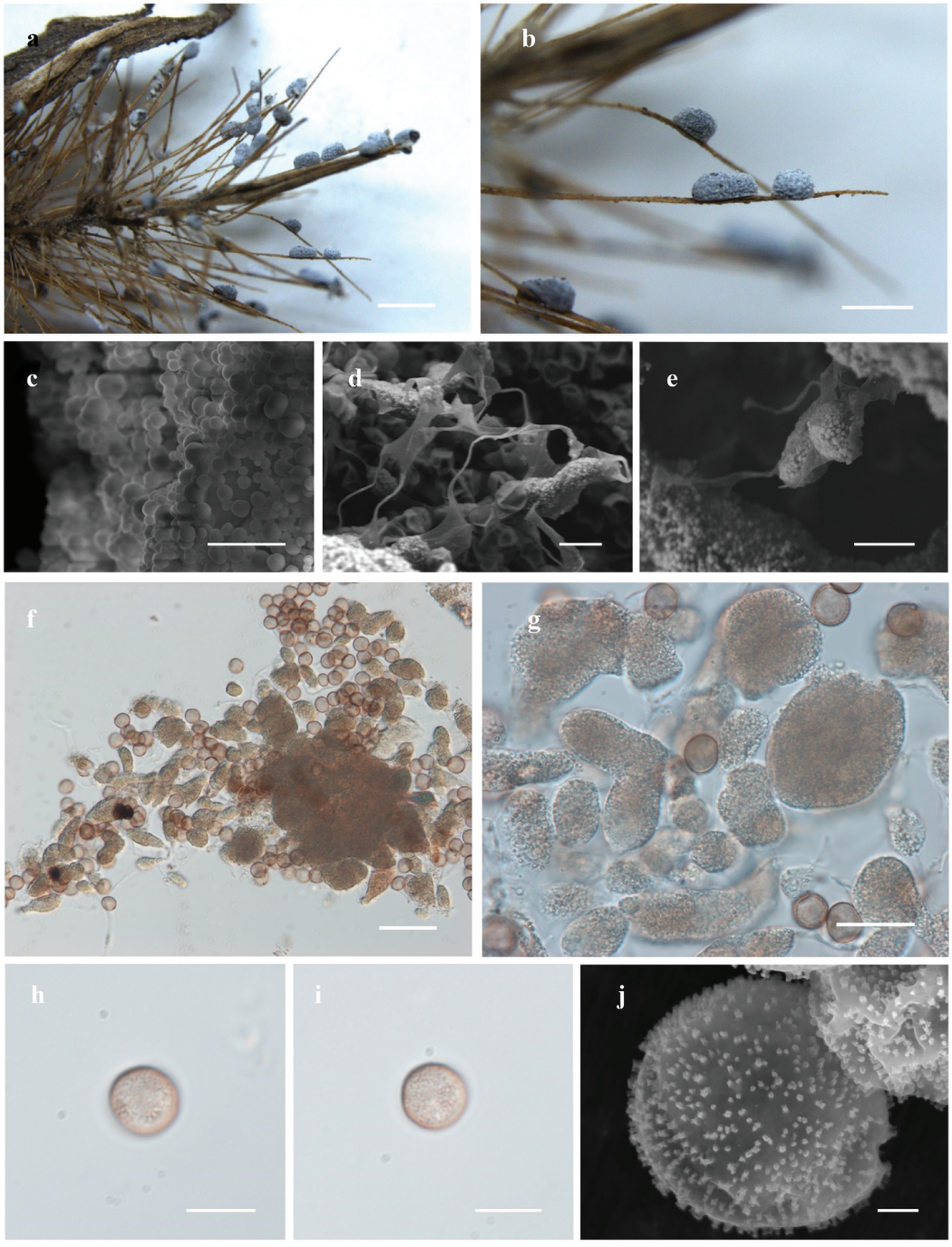

Figure 13. Habitat and microstructure of *Physarum jilinense* (HMJAU M20367). (a, b) Sporocarps. (c) Peridium by SEM. (d–g) Capillitium and lime nodes by SEM and TL. (h–j) Spores by TL and SEM. Scale bars: a = 2 mm; b = 1 mm; c = 4 µm; d, e, h, i = 10 µm; f = 40 µm; g = 20 µm; j= 1 µm.

57262) form a branch with strong support (UBS = 99.3, PP = 1). Although they are grouped together, the genetic distance between them is substantial, confirming the distinctiveness observed in our morphological analysis. Thus, both morphological and phylogenetic evidence support the identification of *P. jilinense* as a new species.

4. Discussion

4.1. Morphological characteristics and phylogenetic relationships of Diderma, Physarum, *and* Neodiderma

In this study, we examined specimens recently collected and preserved at the Jilin Agricultural

University herbarium (HMJAU) spanning nearly 40 years. These specimens were gathered from various regions across China, encompassing 19 provinces. Our investigation confirmed the existence of *Neodiderma* as an independent genus, supported by both morphological observations and phylogenetic analyses. Within the family Didymiaceae, we identified five new *Neodiderma* species: *N. macrosporum*, *N. pseudobisporum*, *N. verrucocapillitium*, *N. rigidocapillitium*, and *N. rufum*.

The newly discovered *Neodiderma* species exhibit distinctive characteristics setting them apart from previously documented species. Similar to *Diderma*, *Neodiderma* species have subglobose sporocarps that are smooth, adorned with amorphous lime granules distributed either loosely or densely. Their capillitium is brown and rough, featuring thickened nodules and enlarged membranous expansions. Interestingly, these species have fewer lime nodes connecting to the capillitium, resembling characteristics observed in *Physarum* species.

It is important to note that the similarity between *Neodiderma* and *Diderma* species may sometimes obscure the reduced presence of lime nodes during observation. However, their characteristic inclusion of lime aligns more with *Physarum* species than with *Diderma*.

We constructed a multi-gene phylogenetic tree using three genes: nSSU, *EF-1α*, and *COI*. However, due to incomplete amplification, not all species within the genus *Neodiderma* were represented by all three genes. Specifically, *Neodiderma macrosporum* (HMJAU M20035-1) was the only species with complete data for all three genes, while *N. pseudobisporum* had sequences for nSSU and *EF-1α*. The remaining species, including *N. rufum*, *N. spumarioides*, and *N. pseudobisporum*, were only represented by nSSU sequences. Despite these limitations, the phylogenetic tree constructed with the available data indicates that *Neodiderma* is placed within the Didymiaceae family and forms sister branches with *Diderma* (Figure 1), although the genetic distance between these genera is significant. Morphologically, *Neodiderma* is characterised by fewer lime knots compared to *Diderma*, which is supported by our phylogenetic analysis. Additionally, the reclassification of *N. ochraceum* and *N. spumarioides* is based on both morphological traits and our updated phylogenetic insights. While *N. spumarioides* shows fewer lime knots, the status of *N. ochraceum* remains uncertain due to incomplete genetic data. As a result, these two species have been reclassified based on the available evidence.

In the genus *Physarum*, we identified 6 new species (*P. guangxiense*, *P. subviride*, *P. nigritum*, *P. biyangense*, *P. neoovoideum*, and *P. jilinense*). Phylogenetic analysis shows that *Neodiderma* is situated between the genera *Physarum* and *Diderma*, sharing characteristics with both. Our comprehensive analysis, integrating morphological observations and phylogenetic insights, suggests that the genus *Neodiderma* represents a transitional group between *Physarum* and *Diderma* (Figure 1), aligning with our initial hypothesis. To further investigate this finding, we plan to expand our specimen collection and conduct more detailed grouping analysis.

4.2. Relationships within the Didymiaceae and Physaraceae

While research on the occurrence and morphological characteristics of myxomycetes has a long history, molecular systematic studies in this group have emerged more recently compared to other eukaryotes. The advent of modern molecular biology techniques has enabled the application of molecular methods to the classification and identification of myxomycetes, providing critical insights into the phylogenetic relationships at the molecular level. These advancements have helped clarify the taxonomic status of several previously ambiguous groups (Feng and Schnittler 2015; Leontyev et al. 2015, 2019, 2022; Feng et al. 2016; Shchepin et al. 2016, 2024; Dagamac et al. 2017; Janik et al. 2020; Bortnikov et al. 2023).

Recently, Prikhodko et al. (2023) conducted a taxonomic revision of species within Didymiaceae using three widely studied genes (nSSU, *EF-1α*, and *COI*). Their results indicated that among the five major genera in the family, only *Diachea* formed monophyletic clades, while the other four genera were polyphyletic or paraphyletic. Consequently, species from the genus *Mucilago* were transferred to *Didymium*, and *L. tigrinum* (Schrad.) Rostaf. was transferred to *Diderma*. In the same year, García-Martín et al. (2023) conducted a more extensive phylogenetic study on the order Physarales, confirming that Didymiaceae is paraphyletic relative to the rest of the order. They also demonstrated that Physaraceae is monophyletic but

that many genera within the family are polyphyletic, reinforcing Prikhodko et al. (2023) conclusions. Additionally, García-Martín et al. (2023) reorganised the genus *Nannengaella* to accommodate *Physarum globuliferum* (Bull.) Pers. and other species with highly calcified sporophores and true calcareous columella. These findings highlight the impact of molecular data on the revision of traditional taxonomy. While these studies have provided more clarity at the order and family levels, some phylogenetic relationships within certain genera remain uncertain. Although we focused on *Physarum*, *Diderma*, and *Neodiderma*, we recognise that a more comprehensive phylogenetic analysis incorporating species from other genera in Physaraceae and Didymiaceae is necessary for a complete understanding of the relationships within these families. The introduction of *Neodiderma* as a new genus is supported by both morphological distinctions and molecular evidence, but we have strengthened the discussion to better articulate these differences.

In our study, we conducted a phylogenetic analysis using three widely studied genes (nSSU, *EF-1α*, and *COI*) alongside detailed morphological research. Although we were unable to obtain sequences for all genes from every species, our results align with previous studies. Specifically, our findings indicate that *Physarum*, *Badhamia*, and *Fuligo* are polyphyletic, which corroborates the results of García-Martín et al. (2023) and earlier research (Nandipati et al. 2012; Cainelli et al. 2020; Ronikier et al. 2022).

In our analysis, we also identified a distinct evolutionary branch that led to the recognition of *Neodiderma* as a newly established genus. This genus includes two previously known species, *N. ochraceum* and *N. spumarioides*, both of which were originally classified under *Diderma*. Through our morphological observations, we noted that *N. spumarioides* displays fewer lime nodes, a feature that aligns more closely with *Neodiderma*, thus supporting its reclassification.

Historically, lime nodes have been a key morphological trait distinguishing between the families Didymiaceae and Physaraceae. Our research suggests that the genus *Neodiderma* exhibits morphological characteristics seen in both *Diderma* and *Physarum*, particularly in its reduced number of lime nodes. Phylogenetically, *Neodiderma* forms a sister clade to *Diderma*, positioning it as a potential transitional genus between Didymiaceae and Physaraceae. This supports our hypothesis that *Neodiderma* serves as a bridge between the two families, reflecting the complexity of taxonomic relationships within Physarales. Our findings provide new insights into the evolution of these genera and underscore the need for further research to fully resolve the relationships between Physaraceae and Didymiaceae. The addition of more molecular data and taxonomic evidence will be crucial to refining these classifications (Figure 1).

5. Conclusions

In this study, we identified *Neodiderma* as a distinct genus based on combined morphological and phylogenetic evidence. Within *Neodiderma* and *Physarum*, we described eleven new species, and proposed a new combination. Our comprehensive analysis, integrating morphological observations and phylogenetic insights, indicates that *Neodiderma* represents a transitional group between Didymiaceae and Physaraceae. These findings provide valuable insights into the internal phylogenetic relationship between Didymiaceae and Physaraceae.

Acknowledgments

We would like to express our sincere gratitude to Huizhong Li and Tolgor Bau for providing the specimens used in this study. We extend our sincere gratitude to Huinan Zhao and Xinya Yang for their invaluable assistance with the examination and organisation of the specimens.

Disclosure statement

No potential conflict of interest was reported by the author(s).

Funding

This work was supported by the National Key R & D of the Ministry of Science and Technology [2023YFD1201601-2], the Jilin Province Science and Technology Development Plan Project [20230202121NC], the National Natural Science Foundation of China [31970020], 111 Program [D17014], and the foundations of Guangdong Provincial Department of Education [2022ZDJS023].

References

Aguilar M, Fiore-Donno AM, Lado C, Cavalier-Smith T. 2014. Using environmental niche models to test the 'everything is everywhere' hypothesis for *Badhamia*. ISME J. 8(4):737–745. doi: 10.1038/ismej.2013.183.

Borg Dahl M, Brejnrod AD, Unterseher M, Hoppe T, Feng Y, Novozhilov Y, Sørensen SJ, Schnittler M. 2018. Genetic barcoding of dark-spored myxomycetes (Amoebozoa)-identification, evaluation and application of a sequence similarity threshold for species differentiation in NGS studies. Mol Ecol Resour. 18 (2):306–318. doi: 10.1111/1755-0998.12725.

Bork P. 2007. Interactive Tree of Life (iTOL): an online tool for phylogenetic tree display and annotation. Bioinformatics. 23(1):127–128. doi: 10.1093/bioinformatics/btl529.

Bortnikov FM, Bortnikova NA, Gmoshinskiy VI, Prikhodko IS, Novozhilov YK. 2023. Additions to *Trichia botrytis* complex (Myxomycetes): 9 new species. Bot Pac. 12(2):1–39. doi: 10.17581/bp.2023.12s03.

Bortnikov FM, Shchepin ON, Gmoshinskiy VI, Prikhodko IS, Novozhilov YK. 2018. *Diderma* velutinum, a new species of *Diderma* (Myxomycetes) with large columella and triple peridium from Russia. Bot Pac. 7(2):47–51. doi: 10.17581/bp.2018.07207.

Cainelli R, de Haan M, Meyer M, Bonkowski M, Fiore-Donno AM. 2020. Phylogeny of Physarida (Amoebozoa, Myxogastria) based on the small-subunit ribosomal RNA gene, redefinition of *Physarum pusillum* s. str. and reinstatement of *P. gravidum* Morgan. J Eukaryot Microbiol. 67(3):327–336. doi: 10.1111/jeu.12783.

Chen SL, Xu F, Yan SZ, Li Y. 2012. Chinese species in the genus physarum and their distribution. Mycosystema. 31(6):845–856.

Chow ZH. 1977. Taxonomic information of Myxomycetes. Changchun: Jilin Agricultural University.

Dagamac NHA, Rojas C, Novozhilov YK, Moreno GH, Schlueter R, Schnittler M. 2017. Speciation in progress? A phylogeographic study among populations of *Hemitrichia serpula* (Myxomycetes). PLoS One. 12(4): e0174825. doi: 10.1371/journal.pone.0174825.

Feng Y, Klahr A, Janik P, Ronikier A, Hoppe T, Novozhilov YK, Schnittler M. 2016. What an intron may tell: several sexual biospecies coexist in *Meriderma* spp. (Myxomycetes). Protist. 167(3):234–253. doi: 10.1016/j.protis.2016.03.003.

Feng Y, Schnittler M. 2015. Sex or no sex? Group I introns and independent marker genes reveal the existence of three sexual but reproductively isolated biospecies in *Trichia varia* (Myxomycetes). Org Divers Evol. 15(4):631–650. doi: 10.1007/s13127-015-0230-x.

Fiore-Donno AM, Berney C, Pawlowski J, Baldauf SL. 2005. Higher-order phylogeny of plasmodial slime molds (Myxogastria) based on elongation factor 1-A and small subunit rRNA gene sequences. J Eukaryot Microbiol. 52 (3):201–210. doi: 10.1111/j.1550-7408.2005.00032.x.

Fiore-Donno AM, Meyer M, Baldauf SL, Pawlowski J. 2008. Evolution of dark-spored Myxomycetes (slime-molds): molecules versus morphology. Mol Phylogenet Evol. 46 (3):878–889. doi: 10.1016/j.ympev.2007.12.011.

Gao Y, Yan SZ, Wang GW, Chen SL. 2018. Two new species and two new records of myxomycetes from subtropical forests in China. Phytotaxa. 350(1):51. doi: 10.11646/phytotaxa.350.1.6.

García-Martín JM, Mosquera J, Lado C. 2018. Morphological and molecular characterization of a new succulenticolous *Physarum* (Myxomycetes, Amoebozoa) with unique polygonal spores linked in chains. Eur J Protistol. 63:13–25. doi: 10.1016/j.ejop.2017.12.004.

García-Martín JM, Zamora JC, Lado C. 2023. Multigene phylogeny of the order Physarales (Myxomycetes, Amoebozoa): shedding light on the dark-spored clade. Persoonia. 51 (1):89–124. doi: 10.3767/persoonia.2023.51.02.

Goloboff PA, Catalano SA, Torres A. 2022. Parsimony analysis of phylogenomic datasets (II): evaluation of PAUP*, MEGA and MPBoot. Cladistics. 38(1):126–146. doi: 10.1111/cla.12476.

Hall T. 1999. BioEdit: a user-friendly biological sequence alignment editor and analysis program for windows 95/98/NT. Nucleic Acids Symp Ser. 41:95–98. doi: 10.1021/bk-1999-0734.ch008.

Hoppe T, Schnittler M. 2015. Characterization of myxomycetes in two different soils by TRFLP-analysis of partial 18S rRNA gene sequences. Mycosphere. 6(2):216–227. doi: 10.5943/MYCOSPHERE/6/2/11.

Janik P, Lado C, Ronikier A. 2020. Range-wide phylogeography of a nivicolous protist *Didymium nivicola* Meyl. (Myxomycetes, Amoebozoa): striking contrasts between the Northern and the Southern Hemisphere. Protist. 171 (6):125771. doi: 10.1016/j.protis.2020.125771.

Kalyaanamoorthy S, Minh BQ, Wong TKF, von Haeseler A, Jermiin LS. 2017. ModelFinder: fast model selection for accurate phylogenetic estimates. Nat Methods. 14:587–589. doi: 10.1038/nmeth.4285.

Katoh K, Standley DM. 2013. MAFFT multiple sequence alignment software version 7: improvements in performance and usability. Mol Biol Evol. 30(4):772–780. doi: 10.1093/molbev/mst010.

Lado C. 2024. An online nomenclatural information system of Eumycetozoa. Real Jardín Botánico, CSIC. Madrid, Spain. http://www.nomen.eumycetozoa.com.2005–2024.

Lado C, Treviño-Zevallos I, García-Martín JM, Wrigley de Basanta D. 2022. *Diachea mitchellii*: a new myxomycete species from high elevation forests in the tropical Andes of Peru. Mycologia. 114(4):798–811. doi: 10.1080/00275514.2022.2072140.

Leontyev D, Buttgereit M, Kochergina A, Shchepin O, Schnittler M. 2022. Two independent genetic markers support separation of the myxomycete *Lycogala epidendrum* into numerous biological species. Mycologia. 115(1):32–43. doi: 10.1080/00275514.2022.2133526.

Leontyev D, Ishchenko Y, Schnittler M. 2023. Fifteen new species from the myxomycete genus *Lycogala*. Mycologia. 115 (4):524–560. doi: 10.1080/00275514.2023.2199109.

Leontyev DV, Schnittler M, Stephenson SL. 2015. A critical revision of the *Tubifera ferruginosa* complex. Mycologia. 107 (5):959–985. doi: 10.3852/14-271.

Leontyev DV, Schnittler M, Stephenson SL, Novozhilov YK. 2019. Systematic revision of the *Tubifera casparyi–T. dictyoderma* complex: resurrection of the genus *Siphoptychium* and introduction of the new genus *Thecotubifera*. Mycologia. 111(6):981–997. doi: 10.1080/00275514.2019.1660842.

Leontyev DV, Schnittler M, Stephenson SL, Novozhilov YK, Shchepin ON. 2019. Towards a phylogenetic classification of the Myxomycetes. Phytotaxa. 399(3):209–238. doi: 10.11646/phytotaxa.399.3.5.

Li XF, Tuo YL, Hu JJ, Li Y, Dai D, Sossah FL, Wang JJ, Guo YF, Liu SY, Ma HX, et al. 2024a. New species, new records, and common species of *Diderma* (Physarales, Didymiaceae) from China. Microbiol Spectr. 2024:e01265-24. doi: 10.1128/spectrum.01265-24.

Li XF, Tuo YL, Li Y, Hu JJ, Sossah FL, Dai D, Liu MH, Guo YF, Zhang B, Li X, et al. 2024b. Two new species of the genus *Diderma* (Physarales, Didymiaceae) in China with an addition to the distribution. J Fungi. 10(8):514. doi: 10.3390/jof10080514.

Li Y, Li HZ, Wang Q, Chen SL. 2008. Flora Fungorum Sinicorum Myxomycetes. Beijing: Science Press.

Lister A. 1925. A monograph of the Mycetozoa. Printed by order of the Trustees of the British Museum 5.

Liu QS, Yan SZ, Chen SL. 2015. Further resolving the phylogeny of Myxogastria (slime molds) based on COI and SSU rRNA genes. Russ J Genet. 51(1):39–45. doi: 10.7868/s0016675814110071.

Liu SL, Zhao P, Cai L, Shen S, Wei HW, Na Q, Han MH, Wei RX, Ge YP, Ma HX, et al. 2024. Catalogue of fungi in China 1. New taxa of plant-inhabiting fungi. Mycology. 1–58. doi: 10.1080/21501203.2024.2316066.

Martin GW, Alexopoulos CJ. 1969. The myxomycetes. Iowa City: University of Iowa Press.

Nandipati SCR, Haugli K, Coucheron DH, Haskins EF, Johansen SD. 2012. Polyphyletic origin of the genus *Physarum* (*Physarales*, Myxomycetes) revealed by nuclear rDNA mini-chromosome analysis and group I intron synapomorphy. BMC Evol Biol. 12(1):1–10. doi: 10.1186/1471-2148-12-166.

Nguyen LT, Schmidt HA, Haeseler AV, Minh BQ. 2015. IQ-TREE: a fast and effective stochastic algorithm for estimating maximum-likelihood phylogenies. Mol Biol Evol. 32(1):268–274. doi: 10.1093/molbev/msu300.

Novozhilov YK, Mitchell DW, Okun MV, Shchepin ON. 2014. New species of *Diderma* from Vietnam. Mycosphere. 5(4):554–564. doi: 10.5943/mycosphere/5/4/8.

Novozhilov YK, Okun MV, Erastova DA, Shchepin ON, Zemlyanskaya IV, García-Carvajal E, Schnittler M. 2013. Description, culture and phylogenetic position of a new xerotolerant species of *Physarum*. Mycologia. 105(6):1535–1546. doi: 10.3852/12-284.

Novozhilov YK, Prikhodko IS, Shchepin ON. 2019. A new species of *Diderma* from Bidoup Nui Ba National Park (southern Vietnam). Protistology. 13:126–132. doi: 10.21685/1680-0826-2019-13-3-2.

Novozhilov YK, Shchepin ON, Prikhodko I, Schnittler M. 2022. A new nivicolous species of *Diderma* (Myxomycetes) from Kamchatka, Russia. Nova Hedwigia: Z fur Kryptogamenkunde. 114(1–2):181–196. doi: 10.1127/nova_hedwigia/2022/0670.

Prikhodko IS, Shchepin ON, Bortnikova NA, Novozhilov YK, Gmoshinskiy VI, Moreno G, Lopez VA, Stephenson SL, Schnittler M. 2023. A three-gene phylogeny supports taxonomic rearrangements in the family Didymiaceae (Myxomycetes). Mycol Prog. 22(2):11. doi: 10.1007/s11557-022-01858-1.

Rao G, Chen SL. 2023. Advancements in the taxonomic study of myxomycetes (Myxogastrea) in China. Mycology. 14(4):316–325. doi: 10.1080/21501203.2023.2255031.

Ronikier A, Janik P, de Haan M, Kuhnt A, Zankowicz M. 2022. Importance of type specimen study for understanding genus boundaries-taxonomic clarifications in *Lepidoderma* based on integrative taxonomy approach leading to resurrection of the old genus *Polyschismium*. Mycologia. 114(6):1008–1031. doi: 10.1080/00275514.2022.2109914.

Ronquist F, Teslenko M, van der Mark P, Ayres DL, Darling A, Höhna S, Larget B, Liu L, Suchard MA, Huelsenbeck JP. 2012. MrBayes 3.2: efficient Bayesian phylogenetic inference and model choice across a large model space. Syst Biol. 61(3):539–542. doi: 10.1093/sysbio/sys029.

Rostafiński JT. 1873. Versuch eines systems der Mycetozoen 9–13. Inaugural dissertation. University of Strassberg, Germany.

Royal BG, Edinburgh. 1969. Flora of British fungi: colour identification chart. Edinburgh (UK): HM Stationery Office.

Shchepin ON, López Villalba Á, Inoue M, Prikhodko IS, Erastova DA, Okun MV, Woyzichovski J, Yajima Y, Gmoshinskiy VI, Moreno G, et al. 2024. DNA barcodes reliably differentiate between nivicolous species of *Diderma* (Myxomycetes, Amoebozoa) and reveal regional differences within Eurasia. Protist. 175(2):126023. doi: 10.1016/j.protis.2024.126023.

Shchepin ON, Novozhilov YK, Schnittler M. 2016. Disentangling the taxonomic structure of the *Lepidoderma chailletii-carestianum* species complex (Myxogastria, Amoebozoa): genetic and morphological aspects. Protistology. 10(4):117–129. doi: 10.21685/1680-0826-2016-10-4-1.

Shchepin O, Novozhilov Y, Woyzichovski J, Bog M, Prikhodko I, Fedorova N, Gmoshinskiy V, Borg Dahl M, Dagamac NHA, Yajima Y, et al. 2022. Genetic structure of the protist *Physarum albescens* (Amoebozoa) revealed by multiple markers and genotyping by sequencing. Mol Ecol. 31(1):372–390. doi: 10.1111/mec.16239.

Shchepin ON, Schnittler M, Erastova DA, Prikhodko IS, Dahl MB, Azarov DV, Chernyaeva EN, Novozhilov YK. 2019. Community of dark-spored myxomycetes in ground litter and soil of taiga forest (Nizhne-Svirskiy Reserve, Russia) revealed by DNA metabarcoding. Fungal Ecol. 39:80–93. doi: 10.1016/j.funeco.2018.11.006.

Song WL, Chen SL. 2024. *Arcyria similaris*: a new myxomycete species from China. Mycologia. 116(3):409–417. doi: 10.1080/00275514.2024.2312077.

Stephenson SL, Schnittler M, Novozhilov YK. 2008. Myxomycete diversity and distribution from the fossil record to the present. Biodivers Conserv. 17(2):285–301. doi: 10.1007/s10531-007-9252-9.

Thompson JD, Gibson TJ, Plewniak F. 1997. The Clustal-X windows interface: flexible strategies for multiple sequence alignment aided by quality analysis tools. Nucleic Acids Res. 63:215–228. doi: 10.1093/nar/25.24.4876.

Walkera G, Silbermanb JD, Karpovc SA, Preisfeld A, Foster P, Frolov AO, Novozhilov Y, Sogin ML. 2003. An ultrastructural and molecular study of *Hyperamoeba dachnaya*, n. sp., and its relationship to the mycetozoan slime moulds. Eur J Protistol. 39(3):319–336. doi: 10.1078/0932-4739-00906.

Wang W, Wang W, Wei SW, Huang W, Qi B, Wang Q, Li Y. 2021. Design of potentially universal SSU primers in myxomycetes using next-generation sequencing. J Microbiol Methods. 184:106203. doi: 10.1016/j.mimet.2021.106203.

Wikmark OG, Haugen P, Lundblad EW, Haugli K, Johansen SD. 2007. The molecular evolution and structural organization of group I introns at position 1389 in nuclear small subunit rDNA of myxomycetes. J Eukaryot Microbiol. 54(1):49–56. doi: 10.1111/j.1550-7408.2006.00145.x.

Zhang B, Ma HX, Li Z, Li Y, Li X. 2020. A new species of *Craterium* (Myxomycetes, Physaraceae) growing on living grass and new records of the genus from China. Phytotaxa. 443(1):13–18. doi: 10.11646/phytotaxa.443.1.2.

Zhao FY, Liu SY, Stephenson SL, Hsiang T, Qi B, Li Z. 2021. Morphological and molecular characterization of the new aethaloid species *Didymium yulii*. Mycologia. 113(5):926–937. doi: 10.1080/00275514.2021.1922224.